AN EXPERIMENTAL INVESTIGATION ON UNIT REYNOLDS NUMBER AND BLUNTNESS EFFECTS ON BOUNDARY-LAYER TRANSITION FOR A 10° HALF-ANGLE CONE AT M_∞

By

Michael Carlton Fischer

Thesis submitted to the Graduate Faculty of the
Virginia Polytechnic Institute
in partial fulfillment for the degree of

MASTER OF SCIENCE

in

MECHANICAL ENGINEERING

June 1969

AN EXPERIMENTAL INVESTIGATION ON UNIT REYNOLDS NUMBER AND BLUNTNESS EFFECTS ON BOUNDARY-LAYER TRANSITION FOR A 10° HALF-ANGLE CONE AT $M_{\infty} = 7$

By

Michael Carlton Fischer

ABSTRACT

An experimental investigation was made of the effect of unit Reynolds number and nose bluntness on the transition Reynolds number for a 10° half-angle cone. The tests were conducted at a nominal Mach number of 7 and the free-stream unit Reynolds number was varied from 1.88×10^6 to 6.21×10^6 per foot. The results showed a significant influence of local unit Reynolds number on transition for the sharp cone. A comparison of data from various facilities on sharp slender cones indicated the presence of unit Reynolds number effects as well as the effect of local Mach number on transition. The present transition data were compared to a correlation based on tunnel noise parameters which showed that radiated tunnel aerodynamic noise had a major influence on the present results. Correlations of the effect of local Mach number on the transition Reynolds number at similar local unit Reynolds numbers are presented. The effect of bluntness was to reduce the local Reynolds number and displace transition rearward completely off the cone surface.

AN EXPERIMENTAL INVESTIGATION ON UNIT REYNOLDS NUMBER AND BLUNTNESS EFFECTS ON BOUNDARY-LAYER TRANSITION FOR A 10° HALF-ANGLE CONE AT $M_{\infty} = 7$

by

Michael Carlton Fischer

Thesis submitted to the Graduate Faculty of the

Virginia Polytechnic Institute

in partial fulfillment for the degree of

MASTER OF SCIENCE

in

Mechanical Engineering

APPROVED:

Chairman, Dr. F. J. Pierce

Dr. R. A. Comparin

Professor C. H. Long

June 1969

Blacksburg, Virginia

TABLE OF CONTENTS

LIST OF FIGURES AND TABLES

PAGE

TABLE

LIST OF SYMBOLS

a	speed of sound
C_F	mean turbulent skin friction coefficient
c	tunnel test section circumference
c_1	tunnel test section circumference used as a reference in Pate and Schueler's correlation
c_f	local skin friction coefficient
c_p	specific heat at constant pressure
h	enthalpy
k	thermal conductivity
L	centerline distance from tunnel throat to model leading edge
M	Mach number
M_{sh}	Mach number at shoulder joining blunt nose and conical frustum
n	exponent in power law relation
N_{St}	Stanton number, $\frac{q}{\rho_\infty u_\infty c_p (T_{aw} - T_w)}$
p	pressure
Pr	Prandtl number
$\dot{q}$	rate of heat flow per unit area
R	gas constant
r_n	nose radius
R	Reynolds number, $\frac{\rho u S}{\mu}$
S	distance along cone surface from stagnation point

S_{sw}	swallowing distance
$(S_{tr})_B$	distance along cone surface from stagnation point to transition location (blunt cone)
$(S_{tr})_S$	distance along cone surface from stagnation point to transition location (sharp cone)
T	temperature
t	time
u	velocity
x	distance along cone axis measured from apex
y	distance perpendicular to cone surface
Δy	wall thickness
$\overline{y}$	the radial distance from cone axis to the location on the bow shock where the shock is essentially conical
γ	ratio of specific heats, 1.4
η	recovery factor
θ_c	cone half-angle
λ	coefficient defined by equation $\mu = \lambda T^{1/2}$
μ	viscosity
ρ	density
$f(\eta)$	dimensionless stream function (value of 2.3 assumed for this investigation)
δ^*	boundary-layer displacement thickness
τ	shearing stress, $\mu \frac{\partial u}{\partial y}$
Φ	cone peripheral angle measured from top ray

Subscripts

aw	adiabatic wall conditions
l	local conditions at boundary-layer edge
s	stagnation heating conditions behind normal shock
t	stagnation conditions
tr	transition
w	wall conditions
∞	free-stream conditions

I. INTRODUCTION

Boundary-layer transition is a common fluid mechanical phenomenon occurring on many configurations at subsonic, supersonic, and hypersonic speeds. Many parameters influence the transition of a laminar boundary layer to a turbulent boundary layer. Such parameters include flow length Reynolds number, local unit Reynolds number, local Mach number, surface roughness, angle of attack, boundary-layer heating or cooling, pressure gradients, nose bluntness, mass addition or removal, and the turbulence level of the free stream.

In recent years, there has been considerable interest in studying transition in the hypersonic speed range encountered by reentry vehicles (see refs. 1 - 6). Boundary-layer transition is undesirable due to the increased skin-friction drag and surface heating associated with a turbulent boundary layer and possible destabilizing effects on the aerodynamic characteristics. Ablation of the protective heat shield may alter the transition location due to effects of nose shape changes, mass addition, and surface roughness.

The purpose of this thesis is to present an experimental investigation of the effects of nose bluntness and unit Reynolds number on boundary-layer transition for a slender cone in a hypersonic free stream. The tests were conducted with a 10° half-angle cone, instrumented for heat transfer, with four interchangeable nose tips. The four tip configurations were one sharp and three with increasing nose radii of $r_n = 0.15$ inch, $r_n = 0.30$ inch, and $r_n = 0.60$ inch.

Free-stream unit Reynolds number varied from 1.88×10^6 to 6.21×10^6 per foot for a range of tunnel stagnation pressures from 185.5 psia to 608.8 psia. The free-stream Mach number varied from 6.82 to 6.86, with tunnel stagnation temperature varying from 1020 R to 1250 R. Schlieren movie frames were taken of each nose tip to define the shock shape.

II. LITERATURE REVIEW

The study of transition of the laminar boundary layer to a turbulent boundary layer is one of the most perplexing problems in fluid mechanics. The classical boundary-layer stability theory for small disturbances was developed for the incompressible case by Tollmien in 1929 and Schlichting in 1933 (see Schlichting, ref. 7).

Experimental confirmation of this theory came in 1943 from the investigation of Schubauer and Skramstad (ref. 8) where the existence of traveling Tollmien-Schlichting waves was proven.

An extension of the small disturbance instability theory to compressible flow for Mach numbers not exceeding 1.5 was made by Lees and Lin (ref. 9) and further refined by Dunn and Lin (ref. 10). The experimental stability work of Laufer and Vrebalovich (ref. 11) at Mach numbers of 1.6 and 2.2 indicated fairly good agreement with the theory of Dunn and Lin, but the revised stability theory of Lees and Reshotko (ref. 12) for Mach numbers up to about 2.5 provided even better agreement with the data of Laufer and Vrebalovich.

In 1958, Demetriades (ref. 13) conducted experimental tests on the stability of the laminar boundary layer at $M = 5.8$ and the results show major disagreement with the theory of Lees and Reshotko. In fact, at present there is no satisfactory compressible flow stability theory for Mach numbers greater than about 3.

Experimental investigations concerning boundary-layer transition on cones were conducted extensively in the 1950's and included both wind tunnel and free-flight results (see refs. 14 - 22). An examination of

the data from these tests revealed a consistent increase in the transition Reynolds number with increasing tunnel stagnation pressure or range pressure which was termed the unit Reynolds number effect. The unit Reynolds number parameter existed in the hypersonic Mach number range also, as reported by Stetson and Rushton (ref. 1), Stainback (ref. 2), Softley, et al. (ref. 4), and others (refs. 5, 6, 23 - 26). The effect of the unit Reynolds number parameter on transition was studied by Whitfield and Potter (ref. 27) and Potter and Whitfield (ref. 28) where it was pointed out that there is an inherent relationship between unit Reynolds number and noise generation from the tunnel wall boundary layer.

Studies by Laufer (refs. 29 and 30) and Vrebalovich (ref. 31) dealing with measurement of noise generation from tunnel wall boundary layers showed that the major source of disturbances in the free stream at the higher Mach numbers ($M_\infty > 3$) was due to radiated pressure fluctuations from the wall boundary layer. Laufer (ref. 29) specifically noted that the radiated noise level was roughly 10 times higher for a turbulent boundary layer as compared to a laminar one.

Recently, Pate and Schueler (ref. 32) presented an empirical correlation of transition Reynolds numbers on flat plates and hollow cylinders through the use of aerodynamic noise parameters. The results indicate that transition was dependent on sound radiation from the turbulent tunnel boundary layer and was not dependent on unit Reynolds number.

On the other hand, correlations based on aerodynamic noise parameters may not be completely suitable since Potter (ref. 33) recently showed a definite unit Reynolds number effect in range free-flight tests

where sound measurements verified that the noise associated with a turbulent tunnel boundary layer was practically nonexistent.

The transition results of this investigation were undoubtedly influenced by radiated noise to some degree, in light of the previous discussion, but since the present study was not directly concerned with noise measurements, there can only be recognition of the possible noise effects on the results.

Another important parameter influencing transition was found to be nose bluntness. Investigations by Moeckel (ref. 34), Diaconis, et al. (ref. 35), Brinich and Sands (ref. 36), and others (refs. 37 - 39) at supersonic Mach numbers showed that the effect of nose bluntness was to displace transition rearward on cones, hollow cylinders, and flat plates. The extent of rearward transition displacement was dependent on the degree of blunting. Brinich and Sands (ref. 36) noted a transition reversal at $M_\infty = 3.1$ when their cone had a flat bluntness. That is, for small amounts of blunting, the location of transition shifted rearward but as the bluntness was increased, the point of transition began to move forward. A transition reversal at a hypersonic Mach number due to nose bluntness was reported by Stetson and Rushton (ref. 1) for a slender cone at $M_\infty = 5.5$. Other data concerning bluntness effects on transition at hypersonic Mach numbers for cones can be found in references 2 - 4 and most recently by Softley (ref. 40).

The reason that transition is shifted rearward when an initially sharp cone (or other body) is blunted is due to the alteration of the flow field due to bluntness. Figure 1 shows a schematic of a blunted cone flow field. The mass flow entering the boundary layer at or nea

the stagnation region has passed through a near-normal shock and consequently is a high entropy flow. The mass flow passing through the shock farther out is essentially unchanged from that of the sharp cone case. Schlieren photographs showing the shock shape for the sharp and blunted tip cone of this study are presented in figures 2(a) through 2(d). The local Mach number and Reynolds number at the boundary-layer edge of a blunt cone are reduced below that of a sharp cone due to the decrease in flow velocity at the boundary-layer edge after passing through the bow shock.

The location downstream of the blunt nose where all of the high entropy flow has been swallowed by the boundary layer and where essentially sharp cone conditions exist is known as the swallowing distance. Various approximations exist for calculating the swallowing distance (see refs. 2, 38, and 41). The method of Zakkay and Krause (ref. 41) will be used for this investigation because it is less complicated and because Stetson and Rushton (ref. 1) used it to obtain successful results.

III. TEST APPARATUS, CONDITIONS, AND PROCEDURE

Description of Model

The model used in this investigation is shown in figure 3. The model was a 10° half-angle cone with four detachable nose tips, an axial length of 12 inches (with sharp tip installed), and a base diameter of 4.23 inches. The cone model was rolled from a 0.063-inch-thick inconel 610 sheet and spun on a lathe to the desired wall thickness of 0.030 inch. Inconel was chosen because of the material's low thermal conductivity which reduces conduction effects and also because it has favorable machining properties.

The detachable nose tips were machined separately from an inconel shaft to obtain uniform wall thicknesses and were threaded to allow for accurate installation on the cone frustum. The blunt tips were elliptical in shape, with the radius at the shoulder joining the stagnation nose region with the conical region being half the radius at the stagnation point, r_n. The dimensions of each tip are as follows:

Nose tip	r_n (in.)	Length (in.)
A	0	2.25
B	0.15	1.75
C	0.30	1.25
D	0.60	0.60

Instrumentation

The model was instrumented with 38 thermocouples for measuring wall temperature and heat-transfer rates. Table 1 lists the thermocouples and gives their surface locations.

All thermocouples were 30-gage (0.010-inch-diameter) chromel-alumel wires which were individually spotwelded to the inside surface of the model skin. The reference temperature of each thermocouple was maintained at about 77 F using a cold junction box.

Test Apparatus

This experimental investigation was conducted in the Langley 11-inch hypersonic tunnel with the Mach 7 air nozzle. The facility is capable of operating over a range of stagnation pressures from 73.5 to 610 psia and a range of free-stream unit Reynolds numbers of 0.8×10^6 to 6.3×10^6 per foot. Free-stream stagnation temperature can be varied over the range of 1000 R to 1280 R, and free-stream Mach number varies from about 6.6 to 6.9 depending on stagnation pressure and length of run. A schematic of the 11-inch facility is shown in figure 4.

Test Conditions and Procedures

For this investigation, a total of 35 runs were made. Seventeen runs were conducted with the sharp tip, and six runs were conducted with each of the three blunt tips. The ranges of tunnel stagnation pressure, stagnation temperature, free-stream Mach number, and free-stream unit Reynolds number were as follows:

P_t, psia	T_t, R	M_∞	R_∞/ft $\times 10^6$
185.5 - 608.8	1020 - 1250	6.82 - 6.86	1.88 - 6.21

Details of the test conditions are given in table 2.

The test procedure consisted of evacuating the test section to a vacuum of about 3 to 4 mm Hg and preheating the test air with an electrical resistance heater. A fast response pressure regulating valve enables steady-state flow conditions to be established in the test section within 2 to 4 seconds.

Each test run was approximately 10 seconds in total length. The test gas passed into an evacuated sphere which later was pumped back down to a vacuum, exhausting the test gas to the atmosphere. After each test run, the model was air cooled in preparation for the next test run.

A temperature time history of each thermocouple was recorded with three 18-channel oscillographs. Stagnation pressure and temperature were recorded separately for each run. In addition, schlieren photographs were taken for each run with a high-speed 70 mm camera to obtain the shock shape.

During the initial positioning of the cone model in the test section, care was taken to align the model precisely at zero angle of attack. The alignment was checked periodically throughout the test investigation to ensure that no misalignment was present.

IV. TEST RESULTS AND DISCUSSION

Heat-Transfer Distribution

Sharp Tip .- Experimental Stanton number distributions (determined by method in appendix A) are compared with laminar and turbulent theory (presented in appendix B) in figures 5(a) through 5(i) for run numbers 1 - 17 (see table 2). For the turbulent theory, the flow was assumed turbulent from the sharp tip.

The beginning of transition in this investigation was taken to be the thermocouple location at which the experimental Stanton numbers first began to deviate consistently and significantly from laminar theory and where this deviation was continued downstream. The end of transition was taken as the highest Stanton number above turbulent theory. An arrow will be used to designate the location of the start and end of transition.

The first 12 test runs presented in figure 5 were made at a wall temperature to total temperature ratio of $T_w/T_t = 0.51$ to 0.53. The last five test runs presented were conducted at a T_w/T_t of 0.45 to 0.47 by increasing the stagnation temperature to determine if there was any effect of a slight variation in T_w/T_t on the transition location.

For the two lowest local unit Reynolds numbers, runs 1 and 2 in figure 5(a), the flow over the cone remained laminar. However, at a local unit Reynolds number of $R_l = 3.46 \times 10^6$ per foot the flow over the rearward portion of the cone became transitional, as indicated by the arrow in figure 5(b).

As the local unit Reynolds number was increased further, the start of transition generally moved forward (figs. 5(c) - 5(d)), and finally, at $R_l = 7.01 \times 10^6$ per foot, fully turbulent flow was established on the rear of the cone (fig. 5(e)).

For the remaining three test runs at $T_w/T_t \approx 0.52$, the location of the start of transition again generally moved forward with increasing local unit Reynolds number, while the location of the end of transition remained stationary except for the last test run (see fig. 5(f)) where the end of transition moved forward.

The first of the five test runs with $T_w/T_t \approx 0.46$ was made at $R_l = 3.77 \times 10^6$ per foot (fig. 5(g)). For this local unit Reynolds number, the start of transition occurred near the base of the cone. As the local unit Reynolds number was increased, the start of transition moved forward somewhat more abruptly than with the tests at $T_w/T_t \approx 0.52$, and fully developed turbulent flow was established only for the highest local unit Reynolds number, $R_l = 6.88 \times 10^6$ per foot (fig. 5(i)).

As indicated in figure 5, there was exceptionally good agreement of measured Stanton number with that of laminar and turbulent theory. In fact, the agreement of the measured heat-transfer data with theory was much better than that of Everhart and Hamilton (ref. 23) where the same theory was used for tests with a slender cone at $M_\infty = 10$.

The results from figure 5 for the $T_w/T_t \approx 0.52$ data show that the start of transition first occurred on the sharp cone model for a local unit Reynolds number of $R_l = 3.46 \times 10^6$ per foot. Increasing the local unit Reynolds number to a maximum of 9.18×10^6 (total of 12 test runs) generally moved the start of transition forward and established

fully turbulent flow on the rearward portion of the cone. Five test runs were conducted at a T_w/T_t of about 0.46 with the start of transition first occurring at $R_l = 3.77 \times 10^6$ per foot. The location of the start of transition moved unhesitantly forward with increasing local unit Reynolds number and fully turbulent flow was established near the cone base for $R_l = 6.88 \times 10^6$ per foot.

Blunt tips.- The experimentally measured heat transfer to the blunted tip configurations, nondimensionalized by the nose stagnation heating rate are presented in figures 6(a) through 6(f) for runs 18 - 35 (see table 2). The heat-transfer distributions are presented as a function of surface distance nondimensionalized by nose radius, S/r_n, and are compared to the laminar theory of Lees (appendix D) for spherically blunted cones. The wall temperature ratio for the blunt cone tests varied over the range of $T_w/T_t = 0.52$ to 0.53.

The heat-transfer results for nose B ($r_n = 0.15$ inch) are presented in figures 6(a) and 6(b). As indicated in the figures, the flow remained laminar and the heating distribution below theory for a range of free-stream unit Reynolds numbers of $R_\infty = 2.01 \times 10^6$ to 6.10×10^6 per foot

The results for nose C ($r_n = 0.30$ inch) are presented in figures 6(c) and 6(d) and, as before, the flow over the cone remained laminar and below theory for a range of free-stream unit Reynolds numbers of $R_\infty = 2.13 \times 10^6$ to 6.08×10^6 per foot.

In figures 6(e) and 6(f), the results with nose D ($r_n = 0.60$ inch) are presented for a range of free-stream unit Reynolds numbers of $R_\infty = 2.10 \times 10^6$ to 6.21×10^6 per foot. As with the other two noses,

the flow remained laminar and the experimental data fell below that of laminar theory.

The reason that the experimental heat-transfer distributions for the blunted configurations fell below the theory of Lees may be due to the fact that the theory of Lees is based on spherically blunted cones. The tips for the present investigation were geometrically blunter than a spherically blunted tip, and since Lees points out that the heat transfer over a sharp slender cone is reduced by spherically blunting the tip, perhaps the greater degree of blunting for the present tests reduced the heat transfer even more.

The results from figure 6 indicate that boundary-layer transition cannot be attained on the blunted cone configurations of this investigation unless free-stream unit Reynolds numbers greater than 6.2×10^6 per foot are reached.

Transition Reynolds Number

Effect of local unit Reynolds number.- The transition Reynolds numbers as determined from the Stanton number distributions of figure 5 are presented in figure 7 as a function of the corresponding local unit Reynolds number.

The circular symbols are the transition Reynolds numbers determined at the start of transition, while the square symbols are the transition Reynolds numbers determined at the end of transition. The open symbols represent the transition Reynolds numbers determined at $T_w/T_t = 0.51$ to 0.53 and the shaded symbols are those determined at $T_w/T_t = 0.45$ to 0.47.

The solid and dashed lines were faired through the data for the start and end of transition and power law relations of the form $R_{S,tr} \propto (R_l/ft)^n$ were calculated. From the figure, it can be seen that there was a stronger effect of local unit Reynolds number on transition Reynolds number for the $T_w/T_t \approx 0.52$ data at the end of transition as compared to the start of transition, which agrees with the results of other investigations (see refs. 23, 25 - 26).

However, the data measured at $T_w/T_t \approx 0.46$ in figure 7 (shaded circular symbols) indicate a less sensitive effect of local unit Reynolds number on the start of transition and presents a completely different picture if considered by itself. Caution must be taken in the interpretation of the $T_w/T_t \approx 0.46$ data. The small reduction in the wall temperature ratio, from $T_w/T_t \approx 0.52$ to 0.46, should not have produced any significant change in the transition Reynolds number.

In fact, all of the data in figure 7 for the start of transition fall within the normal random scatter of experimental results so that no conclusion can be made. Referring to the Stanton number distributions in figure 5, one observes that some variation in determining the location of the start of transition could exist. If this variation was assumed to be no more than three thermocouple locations (0.75 inch) on either side of the previously selected location (arrow) as a maximum (see fig. 5), the transition Reynolds number for the start of transition could be affected by a maximum of about 10 percent.

The transition Reynolds numbers in figure 7 for the start of transition fall within a ± 10 percent scatter. From a comparison of the present data to that of Larson and Mateer (ref. 6), Stainback (ref. 2), Stetson

and Rushton (ref. 1), and Everhart and Hamilton (ref. 23), it was concluded that the scatter of the transition data for this investigation was no more than that normally encountered in transition studies.

In order to determine how the unit Reynolds number effect of this investigation compares with those from studies in other facilities, available cone transition data were collected and are presented in figure 8. The line associated with each data symbol indicates the relationship between transition Reynolds number and local unit Reynolds number. To avoid confusion, only one data symbol for each study was shown. The numbers given for each solid line represent the local Mach number at the boundary-layer edge for the particular investigation.

The references for the data presented are listed in table 3. An attempt was made to choose only data for slender sharp cones at zero angle of attack where the wall temperature to total temperature ratio was $T_w/T_t \approx 0.5$ (present tests). The two references that violated this objective (refs. 3 and 4) were used because they found no effect of wall temperature on transition.

All of the data in figure 8 indicate a substantial effect of local unit Reynolds number on transition Reynolds number except for the data of reference 6 (square symbols). For the case of reference 6 in which a weaker unit Reynolds number effect existed, the explanation for this behavior was attributed to the test facility (Ames 3.5-foot hypersonic tunnel) where cold helium gas was injected into the subsonic portion of the tunnel nozzle for purposes of insulating the wall from the hot free-stream flow. It is known (ref. 42) that the acoustic energy radiated from a jet boundary is a function of the molecular weight of the jet.

Therefore, the low molecular weight helium-air tunnel boundary layer may have influenced the transition results of reference 6.

The unit Reynolds number parameter has never really been established as the most appropriate parameter describing the behavior of transition Reynolds number with increasing tunnel or range pressure. The investigation of Pate and Schueler (ref. 32) showed the dependence of transition Reynolds numbers in conventional wind tunnels on radiated pressure fluctuations from the turbulent tunnel wall boundary layer. The major factors affecting the radiated pressure field were found to be the tunnel wall boundary-layer displacement thickness, the wall mean shear, and the tunnel test section size. Using these factors, an empirical correlation was developed which was independent of unit Reynolds number. The correlation was based on transition data from zero-bluntness flat plate and hollow cylinder models tested in nine different wind tunnels over a free-stream Mach number range of 3 to 8 and a free-stream unit Reynolds number range from 0.6×10^6 to 13.2×10^6 per foot.

The data for the start and end of transition for the present tests are compared with Pate and Schueler's correlation in figure 9. The scatter of the data used for Pate and Schueler's correlation is represented by the dashed lines, and the solid line is their correlation. In order to maintain compatibility, the displacement thickness (δ^*) and the turbulent mean skin-friction coefficient (C_F) were determined for the present study by the same method used by Pate and Schueler. The mean skin-friction coefficient was determined from Van Driest (ref. 43) using the centerline length from the nozzle throat to the cone tip (L) as a characteristic dimension. To determine δ^*, a correlation method

of Maxwell and Jacobs (ref. 44) presented in Pate and Schueler's paper was used. The tunnel circumference (c) for the present tests was 44 inches, and the reference circumference used in the correlation (c_1) was 48 inches.

The data for the start and end of transition from the present tests are above the correlation of Pate and Schueler. It should be mentioned that all of the transition data used by Pate and Schueler was based on the Reynolds number for the end of transition. Therefore, the square symbols of this investigation (end of transition) should be used for comparison purposes. The obvious conclusion here is that since the Reynolds number for transition on cones is greater than that measured on flat plates or hollow cylinders (see Potter, ref. 39) for given free-stream conditions, one would expect the cone data to fall above Pate and Schueler's correlation. However, the slope and general trend of the present data agrees with their correlation which would certainly indicate that there was a major influence of radiated aerodynamic noise on the results of the present investigation.

The correlation of Pate and Schueler is limited to wind tunnels having turbulent wall boundary layers. In addition, as pointed out by Pate and Schueler, the correlation cannot be applied to free-flight results due to the restrictions imposed by C_F and δ^* and also because the correlation is based on finite sized wind tunnels. The recent study by Potter (ref. 33) which showed a definite unit Reynolds number effect in range free-flight tests tends to cast doubt on the correlation of Pate and Schueler. In Potter's tests, noise measurements verified that

the noise levels normally associated with turbulent tunnel wall boundary layers were practically nonexistent.

Clearly, the situation suggests that more investigations must be conducted to determine and define the most appropriate parameters to explain what has been designated the "unit Reynolds number effect, which, by nature, is surely a combination of many interrelated and perhaps still unidentified parameters.

Effect of local Mach number.- Referring to figure 8, it can be seen that there exists a trend between transition Reynolds number and local Mach number. That is, as the local Mach number increases, generally speaking, so does the Reynolds number for transition.

In figure 10(a), the transition data for the present tests are compared with data from the investigations of table 3 to indicate the effect of local Mach number on the start of transition. The vertical line at all but one of the data points with a bar at the top and bottom represent the range of transition Reynolds numbers with unit Reynolds numbers for the particular investigation.

The solid line is the correlation of Softley, et al. (ref. 4) for a local unit Reynolds number of $R_l = 2 \times 10^6$ per foot. The general trend of this curve agrees with correlations of other investigators. For this particular curve, transition Revnolds number is related to local Mach number as $R_{S,tr} \propto M_l^4$.

In contrast, a correlation has been suggested by Larson and Mateer (ref. 6) in which the highest transition Reynolds numbers measured should be used when comparing data from various facilities at similar test conditions in order to assess the effects of various flow variables on

transition. Referring to figure 10(a), the correlation of reference 6 would consider only the highest or the upper bound of the data presented, as represented by the dashed curve. This dependence of transition Reynolds number on local Mach number was constructed, by definition, from data at high local unit Reynolds number which accounts for the deviation from Softley's correlation.

In an attempt to provide further insight into the local Mach number effect on the start of transition, data were taken from figure 10(a) at the same local unit Reynolds number, $R_l = 2.8 \times 10^6$ per foot, and presented in figure 10(b). The data of Larson and Mateer (ref. 6) and Stetson and Rushton (ref. 1) were not included because their transition data were generally higher than those of the remaining investigators. The data of the present investigation were corrected or adjusted to a local unit Reynolds number of 2.8×10^6 by using the relationship $R_{S,tr} \propto (R_l/ft)^{0.604}$ from figure 7. A correction was also applied to the data of reference 4 by using $R_{S,tr} \propto (R_l/ft)^{0.30}$ from their paper.

The faired curve through the selected data points represents the correlation of transition Reynolds number with local Mach number for the present study.

As a further comparison, the correlation of the present investigation is plotted with those of references 4, 23, 25, 26, and 45 in figure 10(c). The correlations are classed into two groups: Those for the start of transition (five curves), and those for the end of transition (three curves). The correlation of the present study (solid curve) agrees reasonably well with those of the other investigators. Note that

the correlations of references 4, 25, and 26 indicate a somewhat different Mach number dependence (bell-shaped curves) from the others.

In the high Mach number range (M_ℓ = 10 to 14), the correlation of the present study agrees considerably well with that of Softley (ref. 4) and Morkovin (ref. 45), but the three curves differ considerably in the range of M_ℓ = 5 to 10.

There appears to be somewhat more uniformity and agreement for the three curves defining the end of transition.

It should be noted that the correlations in figure 10(c) were all made at essentially the same local unit Reynolds number ($R_\ell = 2.0 \times 10^6$ to 2.8×10^6 per foot).

In addition, a comment should be made concerning the obvious fact that each correlation of the type presented in figure 10(c) is constructed using transition data from different facilities where the effects of sidewall sound radiation on the transition measurements undoubtedly vary in magnitude. This sound radiation factor produces a level of uncertainty in comparing transition data from various facilities over a wide Mach number range, but it is an inherent factor which may not be any more significant than the other uncertainties present.

Effect of free-stream unit Reynolds number.- The movement of the surface distance to the start and end of transition with increasing free-stream unit Reynolds number is shown in figure 11. For the open symbols ($T_w/T_t \approx 0.52$) there can be noted two instances of "transition sticking" for the start of transition (S_{tr} = 0.78 and 0.59 ft); that is, transition occurred at the same location as the Reynolds number was increased. For the shaded symbols ($T_w/T_t \approx 0.46$), the location of the start of transition

moved consistently toward the sharp tip with increasing free-stream unit Reynolds number. The data for the end of transition in figure 11 also indicate "transition sticking." As discussed previously, the apparent effect of the small variation in wall temperature ratio on the transition Reynolds number was interpreted as within the scatter of experimental transition data. However, the author believes that these effects were of sufficient interest to be mentioned in passing.

Effects of Nose Bluntness.- As discussed in the literature review, blunting a previously sharp tipped configuration produces many changes in the flow field characteristics. For a cone, the local properties at the edge of the boundary layer are altered such that the local Reynolds number is significantly reduced. As the flow at the boundary-layer edge advances downstream away from the nose region, the local Mach number and Reynolds number increase and approach the equivalent sharp cone conditions. A measure of the distance the flow has to travel before reaching essentially sharp cone conditions is the swallowing distance. Defined in another manner, the swallowing distance is the location on a blunt cone where all of the high entropy flow passing through the curved bow shock has been swallowed by (or has entered) the boundary layer. Using the swallowing distance formulation of appendix C, the local Reynolds number based on surface distance has been calculated for each of the three blunt nose tips at the maximum tunnel conditions tested and are presented in figure 12. Also shown is the local Reynolds number distribution for the sharp tipped cone.

From this figure, it can be seen that the local Reynolds number for the sharp tipped cone reached about 9.2×10^6 at the cone base compared

to about 2.7×10^6 for the tip with $r_n = 0.15$ inch, to as low as 0.68×10^6 for the tip with $r_n = 0.60$ inch. Each of these three Reynolds number distributions for the blunt tips corresponds to the last (maximum tunnel conditions) test run presented in figures 6(b), 6(d), and 6(f) which showed that the flow remained laminar for all three nose tips.

Therefore, the results indicate that in order to attain transitional and turbulent flow over a 10° half-angle cone at $M_l = 5.5$ and at $T_w/T_t \approx 0.5$ with tips of bluntness equivalent to those of this investigation, higher local Reynolds numbers must be attained. This cannot be achieved in the 11-inch facility because the present model dimensions are a maximum for the test section and the maximum stagnation conditions attainable were utilized for the present tests.

The distribution of the local unit Reynolds number along the cone surface for each of the three blunt tips and the sharp tip at the same tunnel conditions of figure 12 are shown in figure 13. The local unit Reynolds number for the sharp tip case is, of course, constant, while the three blunt tip cases are somewhat lower than the sharp tip distribution as were the local Reynolds number distributions of figure 12.

To further indicate the effect of bluntness on local properties, the local Mach number distribution is shown in figure 14. Again, for the sharp tip case, the local Mach number is constant. However, for the blunt tip case, the Mach number varies from zero at the stagnation point behind the normal shock to about 2.25 at the shoulder joining the curved nose region and the conical frustum, and then approaches the sharp tip value far downstream. The local Mach number for $r_n = 0.30$ inch and

r_n = 0.60 inch gradually approach the sharp cone condition at the edge of the boundary layer. This can be explained by the relationship of swallowing distance to nose radius, presented in figure 15.

In figure 15, the swallowing distance is shown to increase significantly with nose radius and, since the swallowing distance is a measure of the distance downstream the flow must travel before approaching sharp cone conditions, the effect of nose bluntness on local properties can be clearly ascertained. For a given cone, increasing the tip radius results in a more predominant bow shock which affects a greater portion of the mass flow entering the shock region (see figs. 2(b) - 2(d)). The properties at the boundary-layer edge downstream of the blunt tip will not reach sharp cone conditions until all of the flow affected by the curved bow shock has entered the boundary layer.

The experimental work of Stetson and Rushton (ref. 1) contains the most recent results concerning nose bluntness transition reversal with a slender cone. Figure 16 is a figure similar to one from their paper which presents the distance to transition for a blunt cone $(S_{tr})_B$, nondimensionalized by the distance to transition for a sharp cone $(S_{tr})_S$, versus the distance to transition for either a blunt or sharp cone S_{tr}, nondimensionalized by the swallowing distance, S_{sw}.

Starting to the right of the figure, the "sharp limit" exists which simply means that all data which fall in that area are for a sharp or essentially sharp cone $(S_{tr}/S_{sw} > 4)$. As the nose tip becomes blunt, S_{sw} begins to increase $(S_{tr}/S_{sw} < 4)$ and the data of reference 1 followed the solid line $\left[(S_{tr})_B/(S_{tr})_S > 1\right]$ for small nose bluntnesses of r_n = 0.031 to 0.25 inch. That is, the location of transition occurred

farther back on the model for small amounts of nose bluntness as compared to the sharp case because of the reduction in local unit Reynolds number. The assumption is made that the local Reynolds number required for transition remains the same for cones with small amounts of nose bluntness as for those with a sharp tip. The nose tip with radius $r_n = 0.15$ inch for the present investigation falls within this range of nose radii. Calculations can thus be made with the present results to explain the behavior of the blunt cone data. From figure 15, a value of swallowing distance for the $r_n = 0.15$ inch nose radius tip was about $S_{sw} = 26$ inches. Based on Stetson and Rushton's results, a slender cone with $r_n = 0.15$ inch should have a value of $S_{tr}/S_{sw} \approx 0.6$. This would result in a distance to transition for the $r_n = 0.15$ inch nose tip cone of $S_{tr} \approx (26)(0.6) \approx 15.6$ inches. Since the cone was only about 11.5 inches in length with the $r_n = 0.15$ inch tip installed, this result verifies that transition should not have occurred on the model. A maximum rearward transition displacement of 4.1 times that of a sharp cone was reached in reference 1 for $r_n = 0.25$ inch.

For increased nose bluntness ($r_n \geq 0.25$ inch), the data of reference 1 followed the upper dashed line in figure 16 and finally approached the "blunt limit" region for $r_n = 1.50$ inches. A departure from the solid line and movement toward the "blunt limit" region signifies a reduction in the critical Reynolds number required for transition. Stetson and Rushton's results show that a typical value of S_{tr}/S_{sw} for a cone with $r_n = 0.30$ inch would be about 0.3. For $r_n = 0.30$ inch figure 15 gives a swallowing distance of about 68 inches so that a distance to transition would be about $S_{tr} \approx (68)(0.3) \approx 20.4$ inches. This

result shows that transition should not have occurred on the model with $r_n = 0.30$ inch. For the $r_n = 0.60$ inch nose radius tip, an approximate value of S_{tr}/S_{sw} from Stetson and Rushton's study would be about 0.07. A swallowing distance from figure 15 for $r_n = 0.60$ inch would be about 170 inches so that an approximate distance to transition would be about $S_{tr} \approx (170)(0.07) \approx 12$ inches. The length of the cone with the $r_n = 0.60$ inch nose tip installed was about 10.5 inches, so that the approximate transition point was slightly rearward of the cone base.

The behavior of the transition point for blunted cones, as mentioned by Stetson and Rushton, appears to be highly dependent on local Mach number. Rogers (ref. 38) conducted bluntness tests at $M_\infty = 3.1$ with a slender cone (lower dashed curve) compared to Stetson and Rushton's value of $M_\infty = 5.5$ and obtained quite different results. The work of Brinich and Sands (ref. 36) at $M_\infty = 3.1$ verifies that of Rogers.

One of the objectives of the present investigation was to obtain transition data with the blunt tipped cone configurations in order to further clarify and define the behavior shown in figure 16. The model of this investigation was the maximum size possible for testing in the 11-inch tunnel. In addition, the maximum Reynolds numbers of the test facility were used in the tests. Therefore, the results show that for the blunt cone configurations of this study, it was not possible to obtain transition on the model for the range of Reynolds numbers tested.

V. CONCLUDING REMARKS

From this experimental investigation of laminar, transitional, and turbulent boundary-layer flow over a sharp and blunt tipped 10° half-angle cone at a nominal free-stream Mach number of 7, it was concluded that:

1. Experimentally measured Stanton numbers on the sharp tipped cone agreed well with laminar and turbulent theory for a range of local unit Reynolds numbers of 2.78×10^6 to 9.18×10^6 per foot.

2. Experimentally measured wall heat-transfer rates on the blunt tipped cone were consistently below that of laminar theory for spherically tipped cones over a range of free-stream unit Reynolds numbers of 2.01×10^6 to 6.21×10^6 per foot.

3. The transition Reynolds numbers for the start and end of transition for the sharp cone at $T_w/T_t \approx 0.52$ displayed a strong effect of local unit Reynolds number. However, transition data determined at $T_w/T_t \approx 0.46$ were less sensitive to local unit Reynolds number, but no positive conclusion was made since the effects noted could be interpreted within the normal scatter of experimental data.

4. A comparison of transition data on slender sharp cones from various facilities at similar test conditions indicates a consistent influence of local unit Reynolds number on the transition Reynolds number. From a comparison of the present data to the correlation of Pate and Schueler (ref. 32), which is based on aerodynamic noise parameters and is independent of unit Reynolds number, it was shown that

radiated aerodynamic noise had a major influence on the transition data of the present investigation.

5. From the comparison of transition data from various facilities, the dependence of transition Reynolds number on local hypersonic Mach number was shown to vary from a minimum at $M_l \approx 5$ and increase sharply with increasing local Mach number. The correlation of transition Reynolds number with local Mach number for the present study was similar to that of other investigations.

6. The location of the start of transition with increasing free-stream unit Reynolds number was shown to generally move forward for the tests conducted with the sharp cone.

7. The local Reynolds number was reduced significantly for the blunt tip cone configurations as compared to the sharp tip case and, assuming the same critical Reynolds number for transition for the blunted cone as for the sharp, the transition delay moved transition completely off the blunted cone surface. Approximate calculations for the rearward shift in transition using Stetson and Rushton's (ref. 1) data indicate that transition on the cone with the three nose tips, r_n = 0.15 inch, 0.30 inch, and 0.60 inch would have occurred at S_{tr} = 15.6 inches, 20.4 inches, and 12 inches, respectively, if the cone had been of sufficient length. These calculations were made for the maximum Reynolds number tested.

VI. SUMMARY

An experimental investigation was made of laminar, transitional, and turbulent boundary-layer flow over a sharp and blunt tipped 10° half-angle cone at a nominal free-stream Mach number of 7. The tests were conducted at stagnation pressures ranging from 185.5 psia to 608.8 psia and for free-stream unit Reynolds numbers of 1.88×10^6 to 6.21×10^6 per foot. Stagnation temperature varied over the range of 1020 R to 1250 R.

Measured Stanton numbers showed good agreement with laminar and turbulent theory for the sharp cone case. The heat-transfer rates measured on the blunt tipped cone configuration were below that of laminar theory for spherically blunted cones. Transition Reynolds numbers for the start and end of transition on the sharp cone indicated a strong dependence on local unit Reynolds number.

By comparing slender sharp cone transition data from various facilities it was shown that the unit Reynolds number effect is a common parameter in many wind tunnels. A comparison of the present data to a correlation based on aerodynamic noise parameters showed the influence of radiated tunnel aerodynamic noise on the present results. The transition data from various facilities also showed a strong dependence on local hypersonic Mach number. A correlation of transition Reynolds number with local Mach number based on the results of the present investigation compared favorably with correlations of other investigations.

For the blunt tip cone configurations, the local Reynolds number was reduced considerably compared to the sharp tip case and transition was delayed to the extent that it did not occur on the cone with any of the blunt tips. This transition delay was approximated by an available method for the three blunt nose tips, r_n = 0.15 inch, 0.30 inch, and 0.60 inch, and the calculations indicated that transition would have occurred at a surface distance of 15.6 inches, 20.4 inches, and 12 inches, respectively (for the maximum unit Reynolds number), if the cone had been of sufficient length.

ACKNOWLEDGMENTS

The author wishes to express his appreciation to Dr. F. J. Pierce, Chairman of the thesis committee, for his assistance and patience while this thesis was being prepared. In addition, the author thanks the other members of the committee: Dr. R. A. Comparin and Professor C. H. Long for their helpful suggestions and criticisms.

Furthermore, the author wishes to thank the National Aeronautics and Space Administration for allowing experimental material obtained from a research project undertaken at the Langley Research Center to be used in this thesis.

Finally, the author wishes to express his gratitude to his wife, Connie, for her patience, understanding, and encouragement during his period of residency at Virginia Polytechnic Institute and for her assistance in the preparation of this thesis.

REFERENCES

1. Stetson, K. F.; and Rushton, G. H.: A Shock Tunnel Investigation of the Effects of Nose Bluntness, Angle of Attack, and Boundary-Layer Cooling on Boundary-Layer Transition at a Mach Number of 5.5. AIAA Paper No. 66-495, June 1966.

2. Stainback, P. Calvin: Some Effects of Roughness and Variable Entropy on Transition at a Mach Number of 8. Presented at the AIAA Fifth Aerospace Sciences Meeting, New York, New York, January 23-25, 1967.

3. Sanator, R. J.; DeCarlo, J. P.; and Torrillo, D. T.: Hypersonic Boundary-Layer Transition Data for a Cold-Wall Slender Cone. AIAA Journal, Vol. 3, No. 4, April 1965, pp. 758-760.

4. Softley, E. J.; Graber, B. C.; and Zempel, R. C.: Experimental Observation of Transition of the Hypersonic Boundary Layer. AIAA Paper No. 68-39, 1968.

5. Maddalon, D. V.; and Henderson, A., Jr.: Boundary-Layer Transition on Sharp Cones at Hypersonic Mach Numbers. AIAA Journal, March 1968, pp. 424-431.

6. Larson, Howard K.; and Mateer, George G.: Transition Measurements on Cones in Hypersonic Flow and Preliminary Observations of Surface Ablation Grooves. Presented at the Boundary-Layer Transition Specialists Study Group Meeting, Aerospace Corporation, San Bernardino, California, July 11-12, 1967.

7. Schlichting, H.: Boundary-Layer Theory. Fourth Edition, McGraw-Hill Book Co., Inc., 1955.

8. Schubauer, G. B.; and Skramstad, H. K.: Laminar-Boundary-Layer Oscillations and Transition on a Flat Plate. NACA Report No. 909, Washington, D. C., 1948.

9. Lees, L.; and Lin, C. C.: Investigation of the Stability of the Laminar Boundary Layer in a Compressible Fluid. NACA TN No. 1115, Washington, D. C., September 1946.

10. Dunn, D. W.; and Lin, C. C.: On the Stability of the Laminar Boundary Layer in a Compressible Fluid. Journal of the Aeronautical Sciences, 22, No. 7, July 1955, pp. 455-477.

11. Laufer, J.; and Vrebalovich, T.: Stability and Transition of a Supersonic Laminar Boundary Layer on an Insulated Flat Plate. Journal of Fluid Mechanics, 9, 1960, pp. 257-299.

12. Lees, L.; and Reshotko, E.: Stability of the Compressible Laminar Boundary Layer. Journal of Fluid Mechanics, 12, 1962, pp. 555-590.

13. Demetriades, A.: An Experimental Investigation of the Hypersonic Laminar Boundary Layer. Journal of Aeronautical Sciences, 25, 1958, pp. 579-600.

14. Lange, A. H.; and Gieseler, L. P.: Measurement of Boundary Transition on a Standard Model to Determine the Relative Disturbance Level in Two Supersonic Wind Tunnels. Naval Ordnance Lab. NAVORD Rep. 2752, February 1953.

15. Evvard, J. C.; Tucker, M.; and Burgess, W. C.: Transition-Point Fluctuations in Supersonic Flow. Presented at 22nd Annual Meeting of the IAS, New York, New York, January 25-29, 1954.

16. Jack, J. R.; and Moskowitz, B.: Experimental Investigation of Temperature Recovery Factors on a 10° Cone at Angle of Attack at a Mach Number of 3.12. NACA TN 3256, July 1954.

17. Michelson, I.: On Laminar, Boundary Layer and Transition in Axially Symmetric Flows. Naval Ordnance Test Station, Tech. Memo. 1611, October 1954.

18. VanDriest, E. R.; and Boison, J. C.: Research on Stability and Transition of the Laminar Boundary Layer. North American Aviation, AL-2196, September 1955.

19. Snodgrass, R. B.: Rocket Research Report No. XX. Flight Measurements of Aerodynamic Heating and Boundary-Layer Transition on the Viking 10 Nose Cone. Naval Research Lab. Rep. 4531, June 1955.

20. Bradfield, W. S.; and DeCoursin, D. G.: Experimental Investigation of Boundary-Layer Transition at Hypersonic Speeds. Rosemont Aero. Labs., University of Minn., Res. Rept. 109, January 1955.

21. Laufer, J.; and Marte, J. E.: Results and a Critical Discussion of Transition-Reynolds-Number Measurements on Insulated Cones and Flat Plates in Supersonic Wind Tunnels. JPL Rept. 20-96, November 1955.

22. Witt, W. R., Jr.: Free-Flight Boundary-Layer Transition Studies on Cones. Proceedings of 4th Midwestern Conf. on Fluid Mech., Purdue University, September 8-9, 1955.

23. Everhart, P. E.; and Hamilton, H. H.: Experimental Investigation of Boundary-Layer Transition on a Cooled 7.5° Total-Angle Cone at Mach 10. NASA TN D-4188, October 1967.

24. Rumsey, C. B.; and Lee, D. B.: Measurements of Aerodynamic Heat Transfer and Boundary-Layer Transition on a 15° Cone in Free Flight at Supersonic Mach Numbers up to 5.2. NASA TN D-888, August 1961.

25. Nagamatsu, H. T.; Sheer, R. E., Jr.; and Graber, B. C.: Hypersonic Laminar Boundary-Layer Transition on 8-Foot-Long, 10° Cone, M = 9.1 - 16. AIAA Journal, Vol. 5, July 1967, pp. 1245-1252.

26. Nagamatsu, H. T.; and Sheer, R. E., Jr.: Boundary-Layer Transition on a Highly Cooled 10° Cone in Hypersonic Flows. General Electric Res. Lab. Rept. No. 64-RL-(3622C), March 1964.

27. Whitfield, J. D.; and Potter, J. L.: The Unit Reynolds Number as a Parameter in Boundary-Layer Stability. AEDC TN-58-77, October 1958.

28. Potter, J. L.: Effects of Unit Reynolds Number, Nose Bluntness, and Roughness on Boundary-Layer Transition. AEDC-TR-60-5, March 1960.

29. Laufer, J.: Aerodynamic Noise in Supersonic Wind Tunnels. Journal of Aeronautical Sciences, 1961, pp. 685-692.

30. Laufer, J.: Some Statistical Properties of the Pressure Field Radiated by a Turbulent Boundary Layer. The Physics of Fluids, Vol. 7, No. 8, August 1964.

31. Vrebalovich, T.: Discussion on Supersonic Wind Tunnels With Low Free-Stream Disturbances, by M. V. Morkovin. Journal of Applied Mechanics, 1960.

32. Pate, S. R.; and Schueler, C. J.: Effects of Radiated Aerodynamic Noise on Model Boundary-Layer Transition in Supersonic and Hypersonic Wind Tunnels. AEDC TR-67-236, March 1968.

33. Potter, J. L.: Observations on the Influence of Ambient Pressure on Boundary-Layer Transition. AEDC-TR-68-36, March 1968.

34. Moeckel, W. E.: Some Effects of Bluntness on Boundary-Layer Transition and Heat Transfer at Supersonic Speeds. NACA Report 1312, 1957.

35. Diaconis, N. S.; Jack, J. R.; and Wisniewski, R. J.: Boundary-Layer Transition at Mach 3.12 as Affected by Cooling and Nose Blunting. NACA TN 3928, January 1957.

36. Brinich, P. F.; and Sands, N.: Effect of Bluntness on Transition for a Cone and a Hollow Cylinder at Mach 3.1. NACA TN 3979, May 1957.

37. Stetson, K. F.: Boundary-Layer Transition on Blunt Bodies With Highly Cooled Boundary Layers. Journal of Aeronautical Sciences, Vol. 27, No. 2, February 1960, pp. 81-91.

38. Rogers, R. H.: Boundary-Layer Development in Supersonic Shear Flow. AGARD Report 269, presented at the Boundary-Layer Research Meeting of the AGARD Fluid Dynamics Panel, London, England, April 25-29, 1960.

39. Potter, J. L.; and Whitfield, J. D.: Effects of Slight Nose Bluntness and Roughness on Boundary-Layer Transition in Supersonic Flows. Journal of Fluid Mechanics, Vol. 12, No. 4, 1962, pp. 501-535.

40. Softley, E. J.: Boundary-Layer Transition on Hypersonic Blunt Slender Cones. AIAA Paper No. 69-705, June 1969.

41. Zakkay, V.; and Krause, E.: Boundary Conditions at the Outer Edge of the Boundary Layer on Blunted Conical Bodies. Aeronautical Research Lab. Rept. 62-386, July 1962.

42. Lighthill, J. J.: Jet Noise. AIAA Journal, Vol. 1, 1963, pp. 1507-1517.

43. VanDriest, E. R.: Turbulent Boundary Layer in Compressible Fluids. Journal of the Aeronautical Sciences, 18, No. 3, 1951, pp. 145-160, 216.

44. Maxwell, H.; and Jacobs, J. L.: Nondimensional Calculation of Turbulent Boundary-Layer Development in Two-Dimensional Nozzles of Supersonic Wind Tunnels. AEDC-TN-61-153, 1962.

45. Morkovin, M. V.: Critical Evaluation of Transition From Laminar to Turbulent Shear Layers With Emphasis on Hypersonically Traveling Bodies. Air Force Flight Dynamics Laboratory, TR-68-149, March 1969.

46. Crocco, L.: The Laminar Boundary-Layer in Gases. North American Aviation, APL, CF-1038, July 1948.

47. VanDriest, E. R.: Turbulent Flows and Heat Transfer. High-Speed Aerodynamics and Jet Propulsion, Vol. V, Princeton University Press, 1959, pp. 372-388.

48. Blasius, H.: The Boundary Layers in Fluids With Little Friction. NACA TM 1256, February 1950.

49. VanDriest, E. R.: Turbulent Boundary Layer on a Cone in A Supersonic Flow at Zero Angle of Attack. Journal of Aeronautical Sciences, Vol. 19, No. 1, January 1952, pp. 55-57, 72.

50. Monaghan, R. J.: An Approximate Solution of the Compressible Laminar Boundary Layer on a Flat Plate. R. and M. No. 2760, Brit. A.R.C., 1953.

51. Monaghan, R. J.: On the Behavior of Boundary Layers at Supersonic Speeds. Fifth International Aero. Conf., Los Angeles, Calif., June 20-23, 1955, Inst. Aero. Sci., Inc., 1955, pp. 277-315.

52. Sims, J. L.: Tables for Supersonic Flow Around Right Circular Cones at Zero Angle of Attack. NASA SP-3004, 1964.

53. Roberts, J. F.; Lewis, C. H.; and Reed, M.: Ideal Gas Spherically Blunted Cone Flow Field Solutions at Hypersonic Conditions. AEDC-TR-66-121, August 1966.

54. Lees, L.: Laminar Heat Transfer Over Blunt-Nosed Bodies at Hypersonic Flight Speeds. Jet Propulsion, April 1956.

BIBLIOGRAPHY

1. Wilkins, M. E.; and Tauber, M. E.: Boundary-Layer Transition on Ablating Cones at Speeds Up to 7 km/sec. AIAA Journal, August 1966, pp. 1344-1348.

2. Mateer, G. G.; and Larson, H. K.: Unusual Boundary-Layer Transition Results on Cones in Hypersonic Flow. Presented at AIAA Sixth Aerospace Sciences Meeting, New York, January 22-24, 1968.

3. McCauley, W. D.; Saydak, A.; and Bueche, J.: The Effect of Controlled Three-Dimensional Roughness on Hypersonic Laminar Boundary-Layer Transition. AIAA Paper No. 66-26, January 1966.

4. Cresci, R. J.; MacKenzie, D. A.; and Libby, P. A.: An Investigation of Laminar, Transitional, and Turbulent Heat Transfer on Blunt Nosed Bodies in Hypersonic Flow. WADC TN 59-119, April 1959.

5. Henderson, A.; Rogallo, R. S.; and Woods, W. C.: Exploratory Hypersonic Boundary-Layer Transition Studies. AIAA Journal, Vol. 3, No. 7, July 1965, pp. 1363-1364.

6. Brinich, P. F.: Effect of Leading-Edge Geometry on Boundary-Layer Transition at Mach 3.1. NACA TN 3659, March 1956.

7. Sheetz, N. W., Jr.: Free-Flight Boundary-Layer Transition Investigations at Hypersonic Speeds. AIAA Paper No. 65-127, January 1965.

8. Richards, B. E.; and Stollery, J. L.: Natural Transition Measurements on a Cold Flat Plate in a Hypersonic Gun Tunnel. Aeronautical Research Council 26405, 1964.

9. Wilson, R. E.: Turbulent Boundary-Layer Characteristics at Supersonic Speeds - Theory and Experiment. Journal Aeronautical Sciences, 17, 1950, pp. 585-594.

10. Schubauer, G. B.; and Klebanoff, P. S.: Contributions on the Mechanics of Boundary-Layer Transition. NACA TN 3489, 1955.

11. Gross, J. F.: Skin Friction and Stability of a Laminar Binary Boundary Layer on a Flat Plate. The Rand Corporation RM-3485-PR, January 1963.

12. Klebanoff, P. S.; Tidstrom, K. D.; and Sargeant, L. H.: The Three-Dimensional Nature of Boundary-Layer Instability. Journal Fluid Mechanics, Vol. 12, Part 1, 1962, pp. 1-34.

13. Betchov, R.: Simplified Analysis of Boundary-Layer Oscillations. Douglas Aircraft Company, Report No. ES 29174, March 1959.

14. Richards, B. E.; and Stollery, J. L.: Transition Reversal on a Flat Plate at Hypersonic Speeds. Proceedings of a Specialists Meeting on Recent Developments in Boundary-Layer Research, AGARDograph 97, Part 1, 1965, pp. 477-601.

15. Potter, J. L.; and Whitfield, J. D.: Boundary-Layer Transition Under Hypersonic Conditions. AEDC-TR-65-99 (AD462716), May 1965.

16. Bertram, M. H.; and Neal, L., Jr.: Recent Experiments in Hypersonic Turbulent Boundary Layers. Presented at the AGARD Specialists Meeting on Recent Developments in Boundary-Layer Research, Naples, Italy, May 10-14, 1965.

17. Eckert, E. R. G.: Engineering Relations for Friction and Heat Transfer to Surfaces in High Velocity Flow. Journal of Aeronautical Sciences, August 1955, pp. 585-587.

18. Reshotko, E.: Stability Theory as a Guide to the Evaluation of Transition Data. AIAA Paper No. 68-669, June 1968.

19. Morkovin, M. V.: On Transition Experiments at Moderate Supersonic Speeds. Journal Aeronautical Sciences, Vol. 24, 1957, p. 480.

20. VanDriest, E. R.; and Boison, J.: Experiments on Boundary-Layer Transition at Supersonic Speeds. Journal Aeronautical Sciences, Vol. 24, December 1957, p. 885.

21. Bertram, M.: Exploratory Investigation of Boundary-Layer Transition on a Hollow Cylinder at a Mach Number of 6.9. NACA TR 1313, 1957.

22. Dorrance, W. H.; and Romig, M. F.: The Effect of Blunting the Nose of a Cone on Conical Surface Reynolds Number and Laminar Flow Heat Transfer at Hypersonic Mach Numbers. Convair Rept. ZA-7-015, March 1955.

23. Holloway, P. F.; and Sterrett, J. R.: Effect of Controlled Surface Roughness on Boundary-Layer Transition and Heat Transfer at Mach Numbers of 4.8 and 6.0. NASA TN D-2054, April 1964.

24. Potter, J. L.; and Whitfield, J. D.: The Relation Between Wall Temperature and the Effect of Roughness on Boundary-Layer Transition. Journal Aerospace Sciences, Vol. 28, 1961, p. 663.

25. Cary, A. M., Jr.: Turbulent Boundary-Layer Heat Transfer and Transition Measurements for Cold-Wall Conditions at Mach 6. AIAA Journal, Vol. 6, 1968, p. 958.

26. Cleary, J. W.: An Experimental and Theoretical Investigation of the Pressure Distribution and Flow Fields of Blunted Cones at Hypersonic Mach Numbers. NASA TN D-2969, 1965.

27. DiCristina, V.: Three-Dimensional Laminar Boundary-Layer Transition on a Sharp 8° Cone at Mach No. 10. AIAA Paper No. 69-12, January 1969.

28. Cleary, J. W.: Effects of Angle of Attack and Nose Bluntness on the Hypersonic Flow Over Cones. AIAA Paper No. 66-414, June 1966.

29. Jones, J. J.: Experimental Investigation of the Heat-Transfer Rate to a Series of 20° Cones of Various Surface Finishes at a Mach Number of 4.95. NASA MEMO 6-10-59L, 1959.

30. Martellucci, A.: Boundary-Layer Transition on a Slender Cone in Hypersonic Flow. AIAA Journal, Vol. 2, No. 4, April 1964, pp. 771-772.

31. Wilson, R. E.: Laminar Boundary-Layer Growth on Slightly Blunted Cones at Hypersonic Speeds. Journal Spacecraft and Rockets, Vol. 2, No. 4, July-August 1965, pp. 490-496.

32. Rufin, I.: Shock Curvature Effect on the Outer Edge Conditions of a Laminar Boundary Layer. AIAA Journal, Vol. 1, No. 12, 1963, pp. 2850-2852.

33. Wilson, D. M.; and Fisher, P. D.: Effect of a Highly Cooled Wall on Hypersonic Turbulent Heat Transfer. NOL TR 65-153, June 1966.

34. Deem, R. E.; and Murphy, J. S.: Flat Plate Boundary-Layer Transition at Hypersonic Speeds. AIAA Paper No. 65-128, January 1965.

35. Michel, R.: Factors Affecting Boundary-Layer Transition at Hypersonic Speeds. Royal Aircraft Establishment Library Translation No. 1073.

36. Howarth, L.: Modern Developments in Fluid Dynamics - High Speed Flow. Vol. I, London, Oxford University Press, 1953.

37. Chapman, D. R.; Kuehn, D. M.; and Larson, H. K.: Investigation of Separated Flows in Supersonic and Subsonic Streams With Emphasis on the Effect of Transition. NACA Rept. 1356, 1958.

38. Palko, R. L.; Burt, R. H.; and Ray, A. D.: An Experimental Investigation of Boundary-Layer Transition on Flat Plates at Mach Number 5, 8, and 10. AEDC Tech Rept. No. AEDC-TDR-64-167, 1964.

39. VanDriest, E. R.: Recent Studies in Boundary-Layer Transition. North American Aviation, Inc., Rept. SID 64-546, 1963.

40. Eckert, E. R. G.: Survey on Heat Transfer at High Speeds. University of Minnesota, ARL 189, 1961.

VITA

Michael Carlton Fischer was born on [redacted], in [redacted] He attended school in the Norfolk area, graduating from Granby High School in June 1959. In September 1959 he enrolled in the Norfolk Division of Virginia Polytechnic Institute to pursue a Bachelor of Science degree in Mechanical Engineering. In the fall of 1961 the author transferred to Virginia Polytechnic Institute and completed his requirements for a Bachelor of Science degree in Mechanical Engineering in August 1963.

Following graduation, he went to work at the Langley Research Center of the National Aeronautics and Space Administration in the Flight Mechanics and Technology Division. In September 1963 the author entered the graduate study program at the Langley Research Center and enrolled in the Mechanical Engineering Department at Virginia Polytechnic Institute as a graduate student in September 1966. Currently, he is in the High Temperature Fluid Mechanics Section of the Aero-Physics Division and is completing his requirements for the Master of Science degree in Mechanical Engineering.

Michael C. Fischer

APPENDIX A

EXPERIMENTAL HEAT-TRANSFER DATA REDUCTION

The convective heat-transfer rate to the cone surface was calculated using the equation:

$$\dot{q}_{conv} = \rho_w c_{pw} \Delta y \frac{dT_w}{dt} \tag{A-1}$$

The value of the wall density ρ_w was taken to be 530 lb/ft^3, and the specific heat varied with the wall temperature as $c_{pw} = 0.1041 + 0.0000335\ T_w$. The thickness of the wall at each thermocouple station was measured and varied over the range from 0.028 to 0.041 inch. The temperature-time derivative dT_w/dt was determined by measuring the slope of each thermocouple trace at the instant constant flow conditions were established in the test section (between 2 and 4 sec). Corrections for radiative heat transfer both from the tunnel wall to the model or from the model to the surrounding environment were insignificant due to the low temperatures encountered (maximum $T_w \approx 120$ F). The heat-transfer measurements were made under nonisothermal wall conditions, with the model wall temperature varying a maximum of about 40 F over the model length. Estimates of the error in the measurements due to heat conduction along the wall were made using the equation for one-dimensional heat conduction in a radial direction along a cone surface:

$$\dot{q}_c = k_w \Delta y \left(\frac{d^2 T_w}{dS^2} + \frac{1}{S} \frac{dT_w}{dS} \right) \tag{A-2}$$

Conduction effects were minimized by the thin skin of the model ($\Delta y \approx 0.030$ in.). The maximum correction due to conduction was calculated to be about 2 percent, with most of the corrections being less than 1 percent of the measured heat-transfer data. For this reason, corrections due to heat conduction effects were neglected.

The adiabatic wall temperature was calculated from the equation:

$$T_{aw} = T_t\left[\eta + \frac{T_\infty}{T_t}(1 - \eta)\right] \tag{A-3}$$

where η is the recovery factor and was taken as $\eta = \sqrt{Pr}$ for laminar flow and $\eta = \sqrt[3]{Pr}$ for turbulent flow. For the range of temperatures encountered in this investigation, the Prandtl number (Pr) varied from 0.710 to 0.729. A value of 0.72 was used for all of the calculations.

The convective heat transfer was converted to a Stanton number by the equation:

$$N_{St} = \frac{\dot{q}}{\rho_\infty u_\infty c_p(T_{aw} - T_w)} \tag{A-4}$$

where a specific heat of $c_p = 0.24$ for air was used.

APPENDIX B

THEORETICAL HEAT TRANSFER

Laminar Theory

The local heat transfer to the cone wall is

$$\dot{q} = \left(k \frac{\partial T}{\partial y} \right)_w \tag{B-1}$$

For a laminar boundary layer, the temperature and velocity profiles have similar shapes at all locations, assuming a uniform wall temperature. That is, both temperature and velocity may be considered as functions of y only. We have

$$\left(\frac{\partial T}{\partial y} \right)_w = \left(\frac{dT}{du} \right)_w \left(\frac{\partial u}{\partial y} \right)_w \tag{B-2}$$

using the relationship

$$\tau_w = \left(\mu \frac{\partial u}{\partial y} \right)_w \tag{B-3}$$

we have

$$\dot{q} = \tau_w \left(\frac{k}{\mu} \right)_w \left(\frac{dT}{du} \right)_w \tag{B-4}$$

From the expression for Stanton number

$$N_{St} = \frac{\dot{q}}{\rho_\infty u_\infty c_p (T_{aw} - T_w)} \tag{B-5}$$

and by substituting equation (B-4) into (B-5) we have an expression for the local Stanton number

$$N_{St} = \frac{c_f}{2Pr_w^{2/3}} \tag{B-6}$$

where

$$c_f = \frac{\tau_w}{1/2\ \rho_\infty u_\infty^2} \tag{B-7}$$

$$Pr_w = \left(\frac{c_p \mu}{k}\right)_w \tag{B-8}$$

Equation (B-6) expresses a relationship between heat transfer and skin-friction and is known as the Reynolds analogy. Crocco (ref. 46) and VanDriest (ref. 47) both developed similar expressions for the Reynolds analogy.

Blasius (ref. 48) developed an expression for the local skin-friction on a flat plate in laminar flow as

$$c_f = \frac{0.664}{\sqrt{R_S}} \tag{B-9}$$

which combined with the Reynolds analogy gives

$$N_{St} = \frac{0.332}{Pr_w^{2/3}\sqrt{R_S}} \tag{B-10}$$

From VanDriest (ref. 49) the local Stanton number for axially symmetric laminar flow over a sharp cone is $\sqrt{3}$ times that for a flat plate at the same local Reynolds number, Mach number, and wall temperature to local free-stream temperature ratio.

Rewriting equation (B-10) for the laminar heat transfer to a cone in terms of free-stream conditions, introducing a reference temperature, and assuming $Pr = 0.72$, we have

$$N_{St_\infty} = 4.317 \frac{T_l^{1/4}}{p_\infty M_\infty} \sqrt{\frac{p_l M_l \mu' T_\infty}{ST'}} \tag{B-11}$$

where a reference temperature defined by Monaghan (ref. 50) was used

$$\frac{T'}{T_l} = 0.575\left(\frac{T_w}{T_l}\right) + 0.425 + 0.0328\, M_l^2 \tag{B-12}$$

Turbulent Theory

For turbulent theory, the same relationship between local Stanton number and skin friction holds true (eq. (B-6)). Schlichting (ref. 7) gives the following expression for the local skin friction for turbulent flow on a flat plate

$$c_f = \frac{0.0592}{(R_S)^{1/5}} \tag{B-13}$$

which combined with the Reynolds analogy gives

$$N_{St} = \frac{0.0296}{Pr_w^{2/3}(R_S)^{1/5}} \tag{B-14}$$

For turbulent axisymmetric flow over a cone, the local Stanton number is 1.15 times the value for a flat plate under the same turbulent local conditions (ref. 49).

Introducing a reference temperature, and converting to free-stream conditions, assuming $Pr = 0.72$, the following expression for the turbulent free-stream Stanton number for a cone is developed

$$N_{St_\infty} = 0.088\left(\frac{p_l M_l \sqrt{T_l}}{T'}\right)^{4/5} \frac{T_\infty}{p_\infty M_\infty}\left(\frac{\mu'}{S}\right)^{1/5} \tag{B-15}$$

where the following reference temperature for turbulent flow was used (ref. 51)

$$\frac{T'}{T_l} = 0.54\,\frac{T_w}{T_l} + 0.46 + 0.0284\,M_l^2 \tag{B-16}$$

APPENDIX C

SWALLOWING DISTANCE AND DEVELOPMENT OF LOCAL PROPERTIES

A convenient method for computing approximate local properties along blunted cones involves the use of the swallowing distance, S_{sw}. The swallowing distance is defined as the position on the cone where the high entropy flow which has passed through the curved region of the bow shock has been swallowed by the boundary layer. At this location, the properties at the boundary-layer edge are essentially the same as that for an equivalent sharp cone.

A formulation for the swallowing distance was developed by Zakkay and Krause (ref. 41) by assuming a linear Mach number gradient along the boundary-layer edge. Their subsequent expression for the swallowing distance is of the form

$$S_{sw} = r_n\left[\frac{3}{2}\,\frac{\sqrt{R/\gamma}}{\lambda p_l}\,\frac{\rho_\infty^2 u_\infty^2}{(3M_l + M_{sh})}\,\frac{\bar{y}^4 r_n}{f^2(\eta)\,\sin^2\theta_c}\right]^{1/3} \qquad (C\text{-}1)$$

The transformed stream function, $f(\eta)$, was assumed to have a value of 2.3 after reference 1. Values of the local Mach number, M_l, and the Mach number at the shoulder joining the blunt nose with the conical frustum, M_{sh}, were obtained from the tables of references 52 and 53, respectively. Surface pressure, p_l, for the blunt cone was assumed to be constant and equal to the equivalent sharp cone pressure.

The shock shape was obtained from schlieren photographs and $\bar{y}$ was taken to be the radial distance from the cone axis to the shock location

where the pressure recovery across the shock was of such a value that expansion to p_l resulted in 0.95 M_l. The local flow properties approach sharp cone conditions asymtotically from the swallowing distance. Therefore, the swallowing distance can be computed from equation (C-1). Since this distance represents the location where the local Mach number is 0.95 M_l for a sharp cone (known value), the local Mach number distributions along the blunt cone surface can be determined by assuming a linear gradient from M_{sh} to 0.95 M_l.

Once the local Mach number distribution is known, the energy equation can be written

$$H_t = h_l + \frac{u_l^2}{2} \tag{C-2}$$

or, for a perfect gas

$$H_t = c_p T_l + \frac{(M_l)^2(\gamma \mathcal{R}_g T_l)}{2} \tag{C-3}$$

solving for T_l, we have

$$T_l = \frac{H_t}{\left(c_p + \frac{\gamma \mathcal{R}_g M_l^2}{2}\right)} \tag{C-4}$$

Values of T_l for corresponding values of M_l can now be computed. From these values of T_l, the speed of sound a_l, u_l, ρ_l, and μ_l can be determined, thus enabling the local Reynolds number, $R_l = \frac{\rho_l u_l S}{\mu_l}$, to be calculated.

Free-stream properties were computed assuming an isentropic expansion ($\gamma = 1.4$) from the known stagnation conditions. For the sharp cone case, local properties at the boundary-layer edge were computed from the tables of Sims (ref. 52).

APPENDIX D

LAMINAR HEAT TRANSFER OVER SPHERICALLY TIPPED CONES

The theory used for the heat transfer over the blunt-nosed cones of this investigation is that of Lees (ref. 54) which is expressed as

$$\frac{\dot{q}_w}{\dot{q}_s} = A(\theta_c) \frac{\cot \theta_c + \left[\frac{S}{r_n} - \left(\frac{\pi}{2} - \theta_c\right)\right]}{\left\{B(\theta_c) + \left(\cot \theta_c + \left[\frac{S}{r_n} - \left(\frac{\pi}{2} - \theta_c\right)\right]\right)^3\right\}^{1/2}} \qquad \text{(D-1)}$$

where:

$$A(\theta_c) = \frac{\sqrt{3}}{2}\left[\left(1 - \frac{1}{\gamma_\infty M_\infty^2}\right) \sin^2\theta_c + \frac{1}{\gamma_\infty M_\infty^2}\right]^{1/2} \sqrt{\frac{\pi}{2} - \theta_c}$$

$$B(\theta_c) = \frac{0.1875}{\sin^2\theta_c \left\{\left[1 - \left(\frac{1}{\gamma_\infty M_\infty^2}\right)\right] \sin^2\theta_c + \left(\frac{1}{\gamma_\infty M_\infty^2}\right)\right\}} \frac{D(\theta)}{\theta} - \cot^3\theta_c$$

$$D(\theta) = \left(1 - \frac{1}{\gamma_\infty M_\infty^2}\right)\left(\theta^2 - \frac{\theta \sin 4\theta}{2} + \frac{1 - \cos 4\theta}{8}\right) + \frac{4}{\gamma_\infty M_\infty^2}\left(\theta^2 - \theta \sin 2\theta + \frac{1 - \cos 2\theta}{2}\right) \cdots$$

θ_c = cone half-angle, radians

$\theta = \frac{\pi}{2} - \theta_c$

S/r_n = surface distance from stagnation point nondimensionalized by nose radius.

For the conditions of the present test, $\theta_c = 10^\circ$ (0.1744 radians), $M_\infty = 6.86$, and $\gamma_\infty = 1.4$, we have

$$\frac{\dot{q}_w}{\dot{q}_s} = (0.2164) \frac{5.671 + \left[\frac{S}{r_n} - 1.395\right]}{\left[63.7 + \left(5.671 + \left[\frac{S}{r_n} - 1.395\right]\right)^3\right]^{1/2}} \qquad \text{(D-2)}$$

Fluid which has passed through a near normal shock.

2. Fluid which has passed through essentially a conical shock

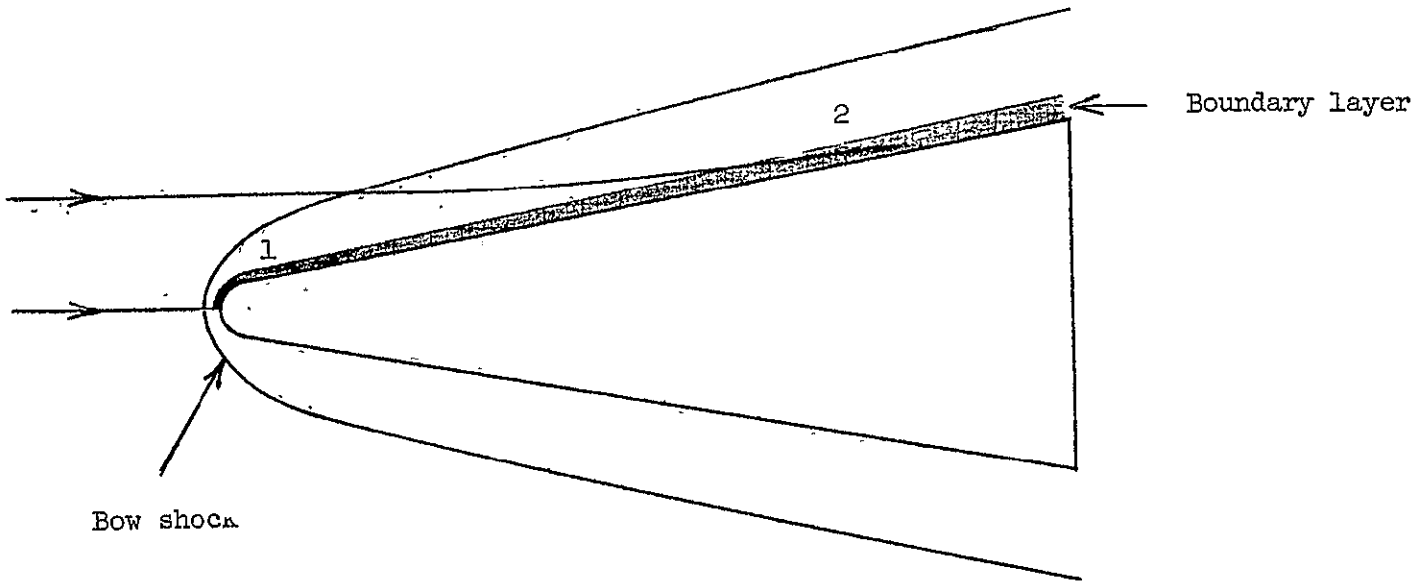

Figure 1.- Flow past a blunted cone.

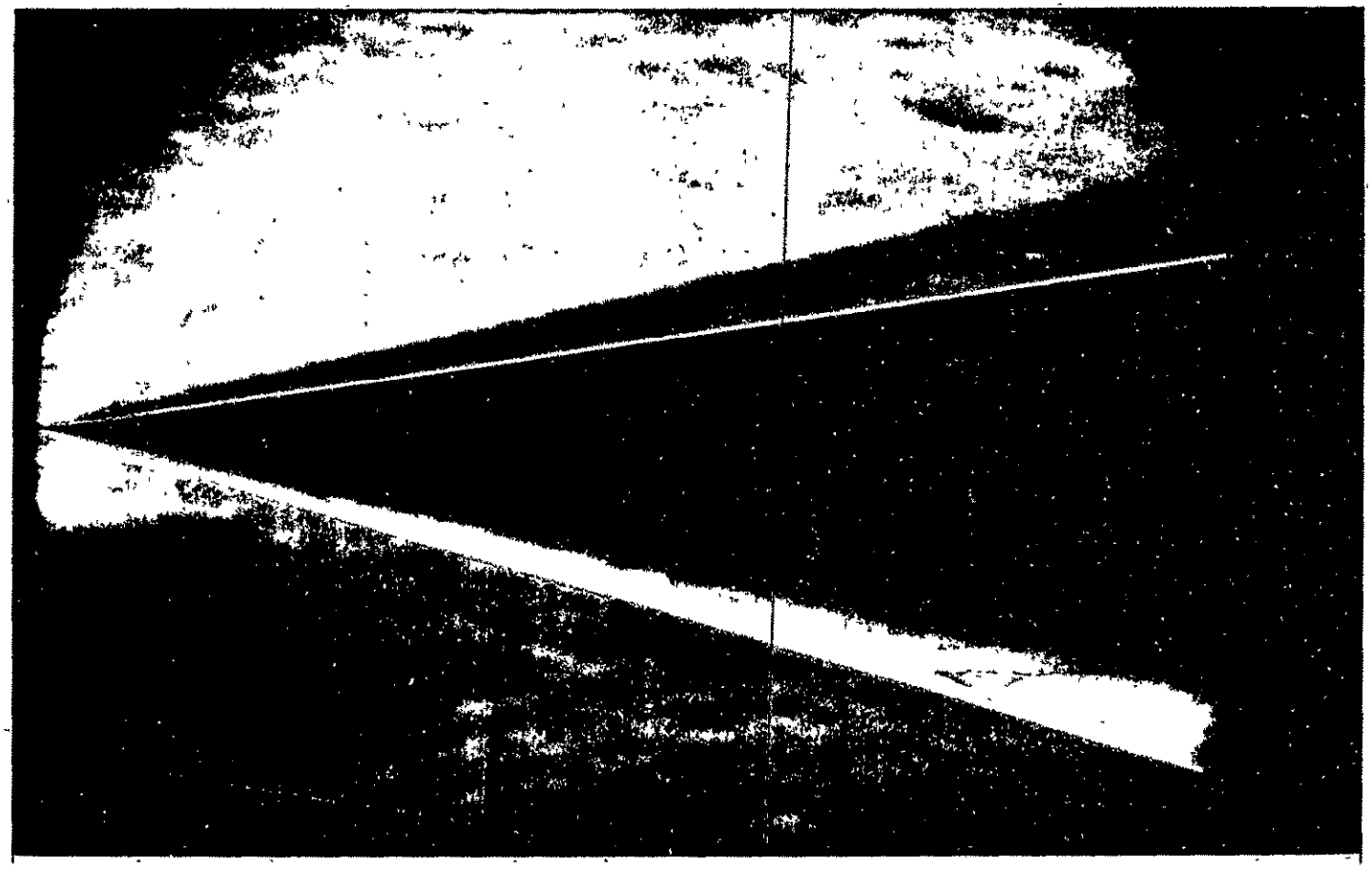

(a) Nose A.

Figure 2.- Schlieren photographs of model.

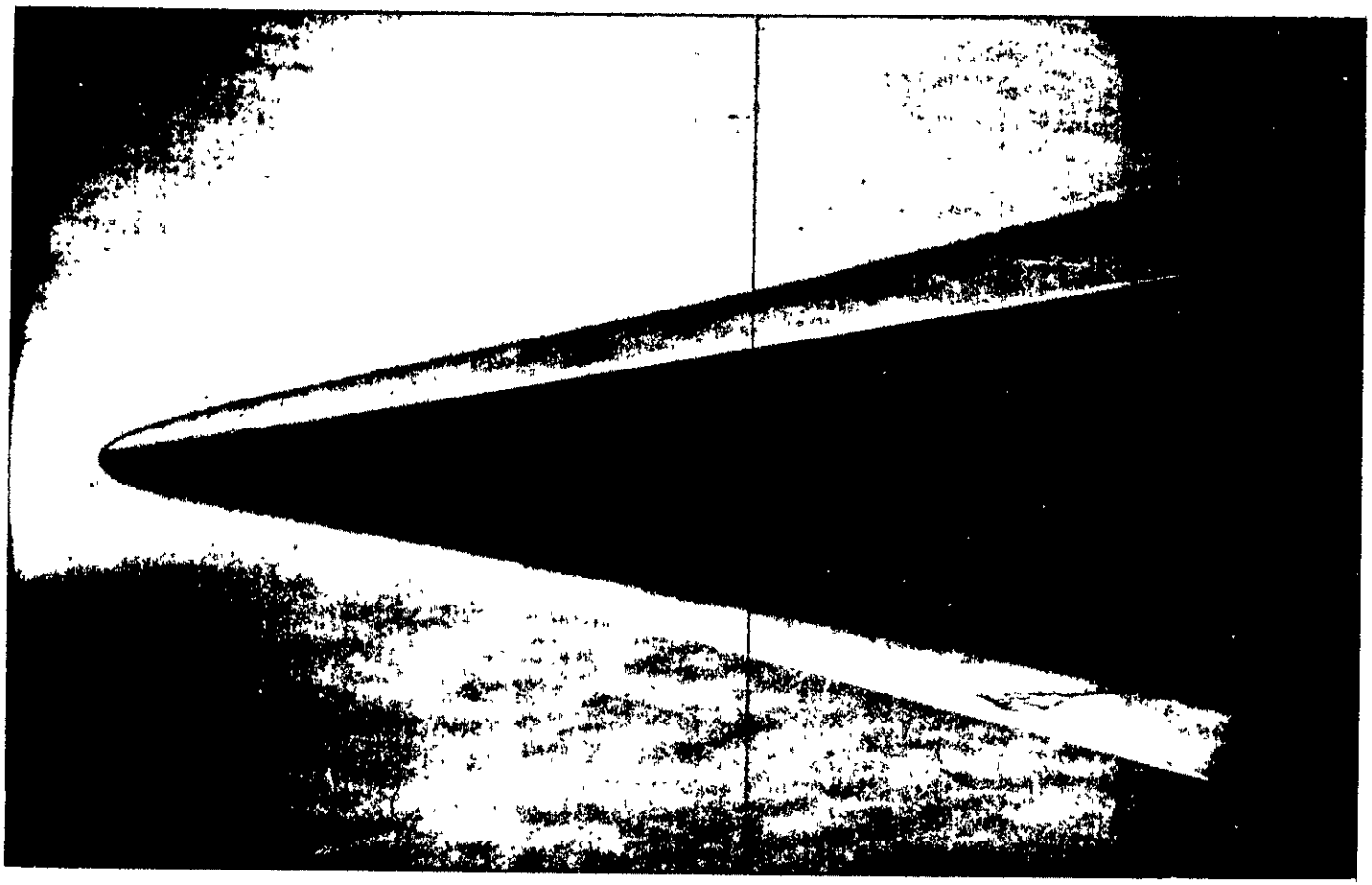

(b) Nose B.

Figure 2.- Continued.

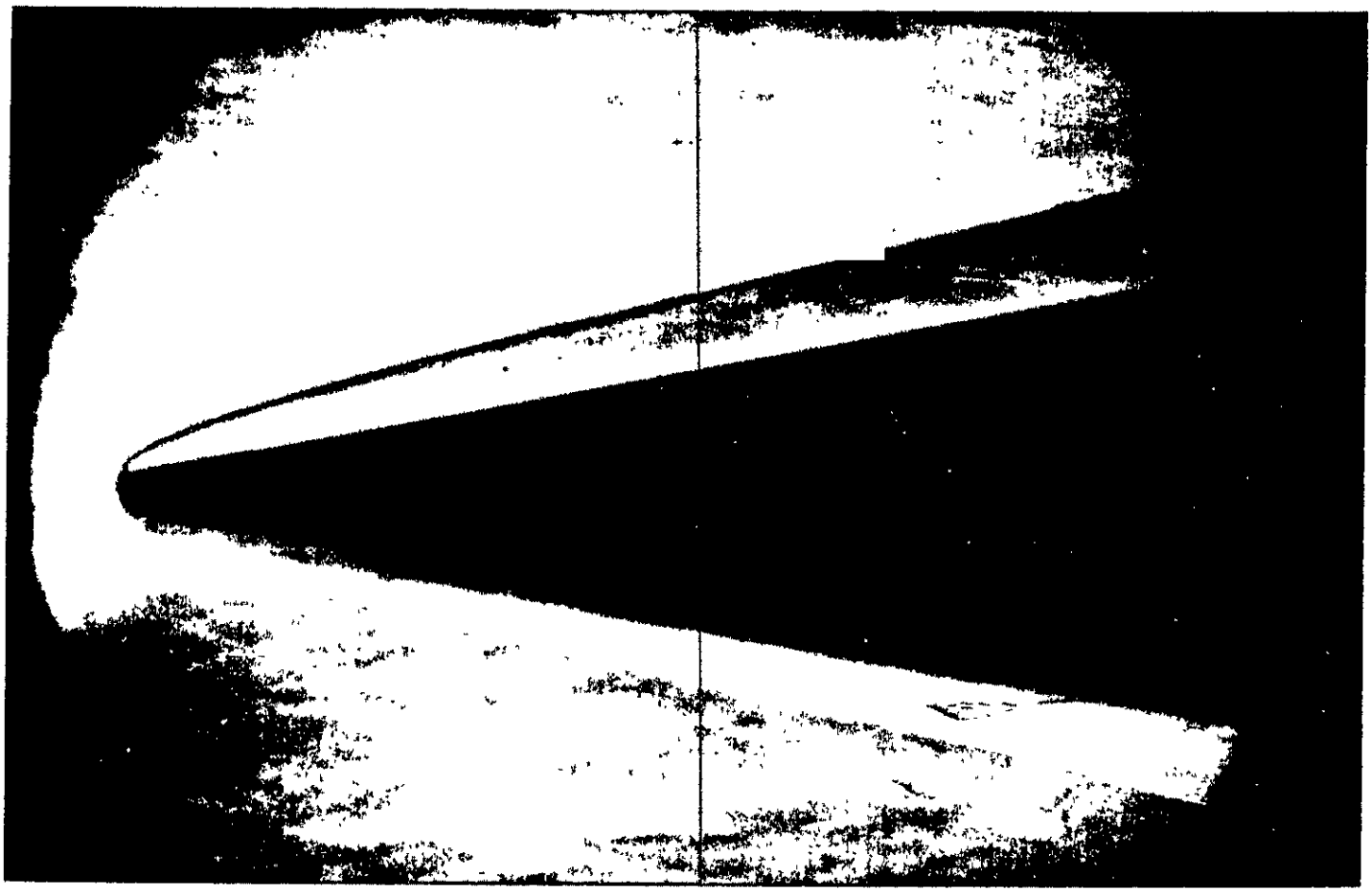

(c) Nose C.

Figure 2.- Continued.

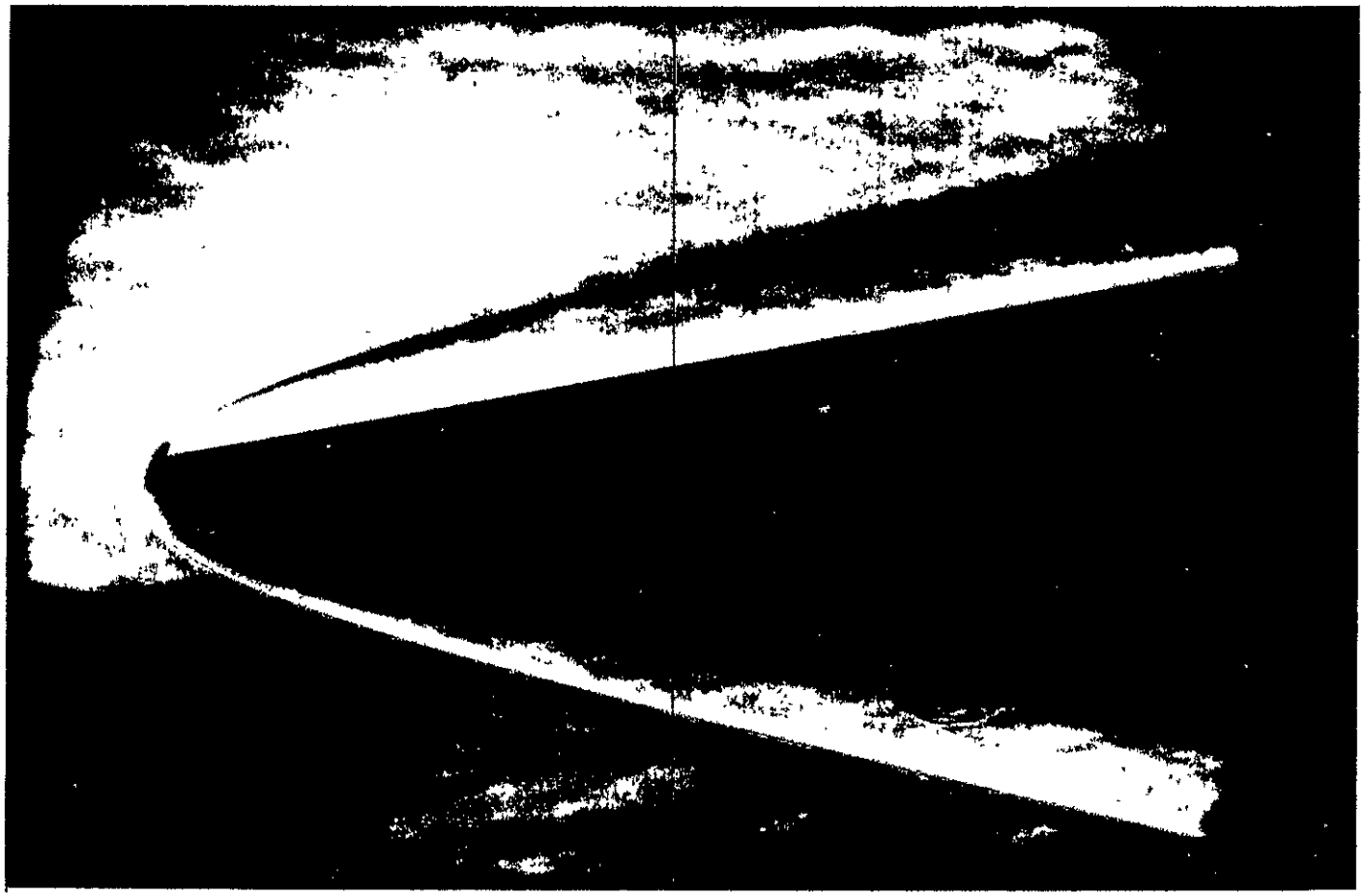

(d) Nose D.

Figure 2.- Concluded.

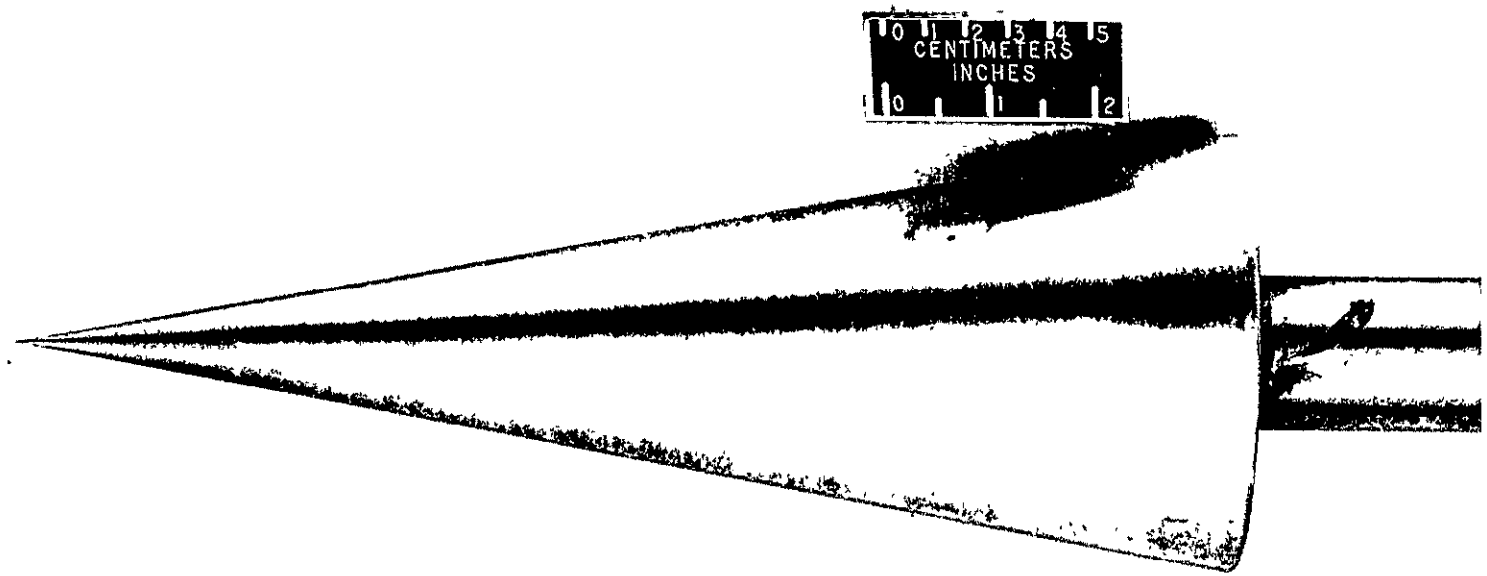

(a) Sharp cone configuration.

Figure 3.- Photograph of model.

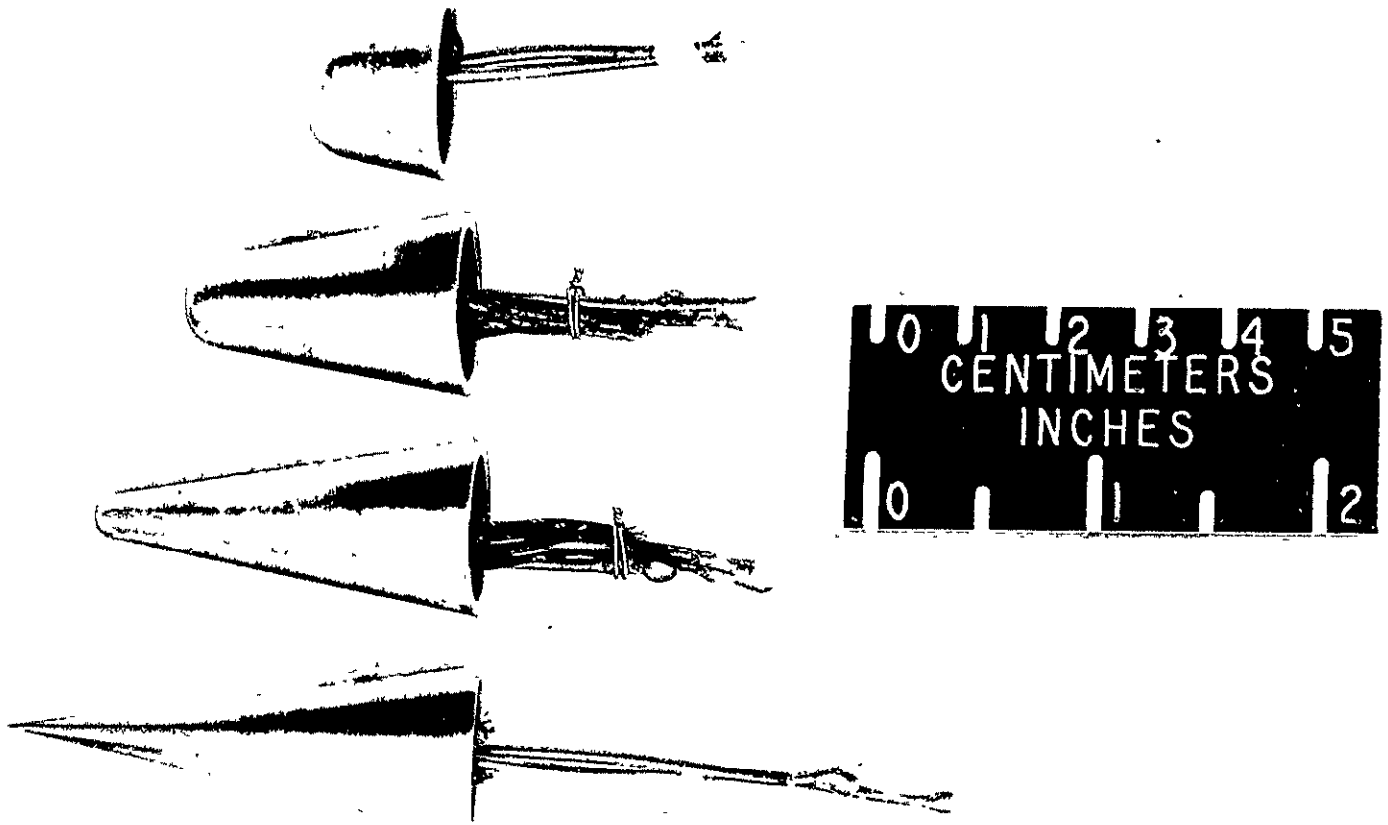

(b) Sharp and blunt nose tips.

Figure 3.- Concluded.

TABLE 1.- THERMOCOUPLE LOCATIONS ON INSTRUMENTED CONE MODEL

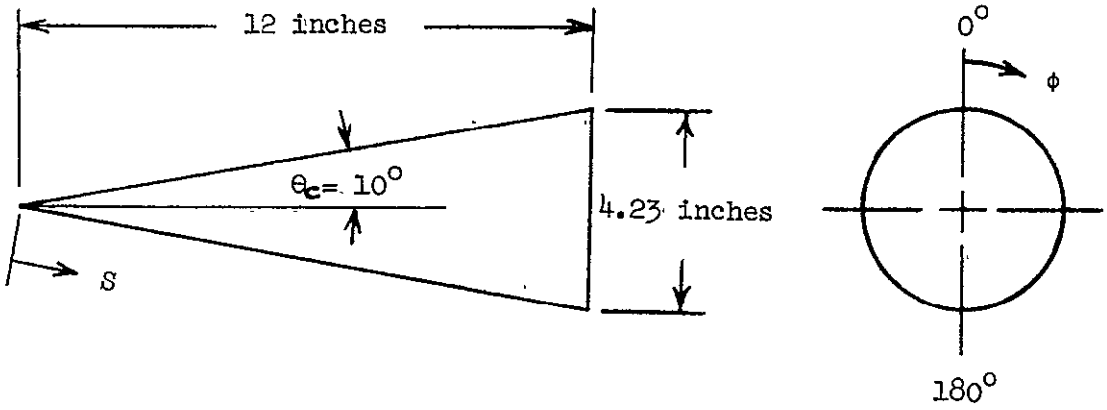

THERMOCOUPLE	S IN.	ϕ DEG.	THERMOCOUPLE	S IN.	ϕ DEG.
1	2.48	0	20	7.13	0
2	2.68	↓	21	7.38	↓
3	2.88		22	7.63	
4	3.13		23	7.88	
5	3.38		24	8.18	
6	3.63		25	8.38	
7	3.88		26	8.63	
8	4.13		27	8.88	
9	4.38		28	9.13	
10	4.63		29	9.38	
11	4.88		30	9.63	
12	5.13		31	9.88	
13	5.38		32	10.13	
14	5.63		33	10.38	
15	5.88		34	10.63	
16	6.13		35	10.88	
17	6.38		36	11.13	
18	6.63		37	11.38	
19	6.88		38	11.63	

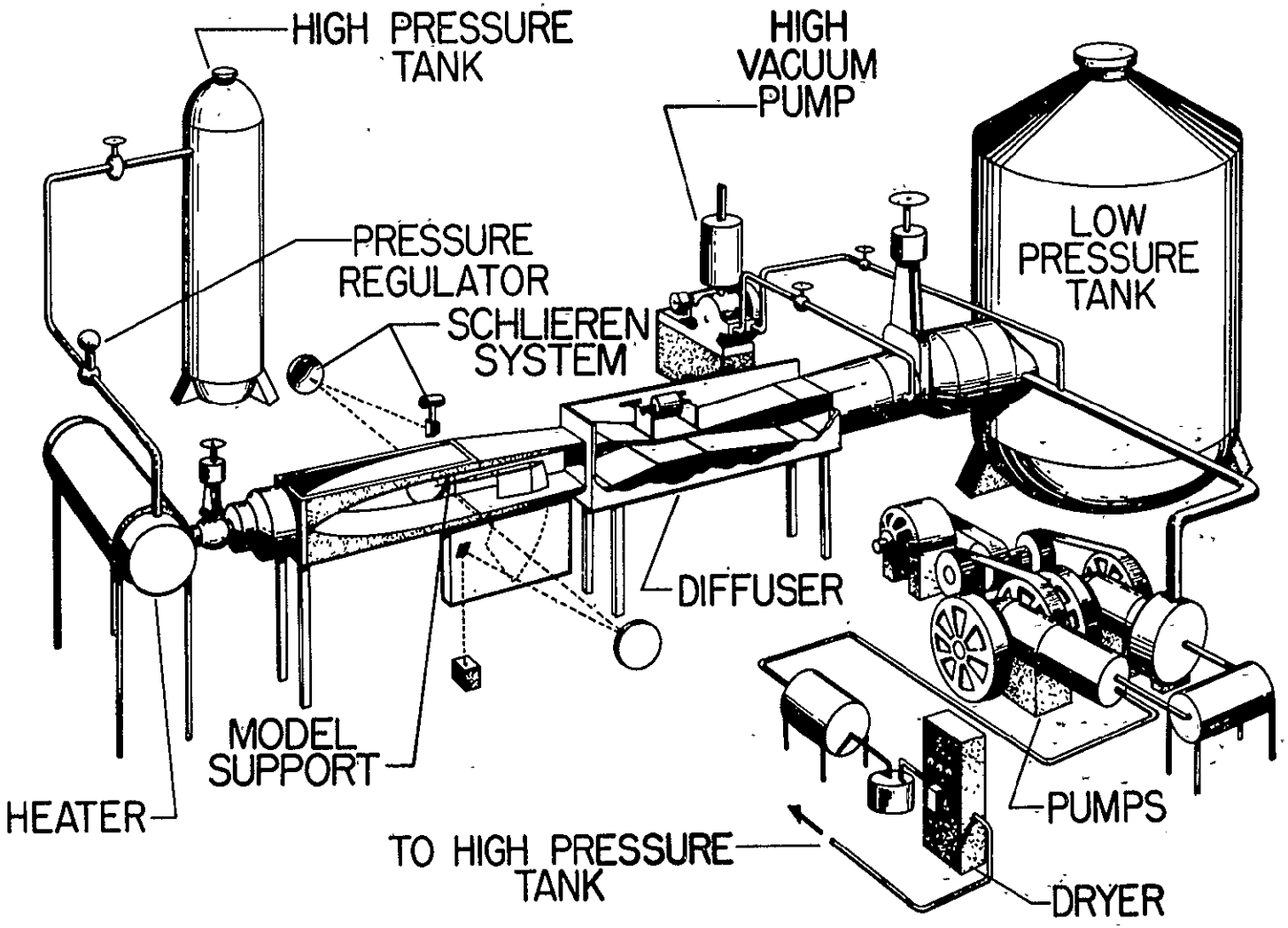

Figure 4.- Schematic of Langley 11-inch facility.

TABLE 2.- TEST CONDITIONS OF EXPERIMENTAL INVESTIGATION

Run number	Stagnation pressure psia	Stagnation temperature ^{o}R	Free-stream Mach number	Free-stream unit Reynolds No. per foot
		NOSE A (SHARP)		
1	185.5	1055	6.82	1.88×10^{6}
2	201.0	1060	6.82	2.02
3	226.3	1040	6.82	2.34
4	255.9	1035	6.83	2.66
5	288.0	1050	6.84	2.91
6	360.0	1060	6.85	3.58
7	404.0	1055	6.86	4.02
8	439.0	1040	6.86	4.52
9	482.0	1070	6.86	4.70
10	519.0	1075	6.86	5.01
11	546.7	1070	6.86	5.33
12	608.8	1043	6.86	6.21
13	301.3	1180	6.84	2.53
14	368.3	1194	6.85	3.03
15	437.0	1200	6.86	3.56
16	516.0	1225	6.86	4.07
17	604.0	1250	6.86	4.61

TABLE 2.- Continued

Run number	Stagnation pressure psia	Stagnation temperature °R	Free-stream Mach number	Free-stream unit Reynolds No. per foot
		NOSE B (r_n = 0.15 in.)		
18	197.4	1050	6.82	2.01×10^6
19	294.0	1050	6.84	2.99
20	369.2	1035	6.85	3.80
21	423.5	1025	6.86	4.43
22	516.0	1068	6.86	5.06
23	607.5	1050	6.86	6.10
		NOSE C (r_n = 0.30 in.)		
24	200.2	1020	6.82	2.13×10^6
25	288.4	1060	6.84	2.88
26	363.0	1050	6.85	3.67
27	434.5	1055	6.86	4.36
28	520.0	1080	6.86	4.98
29	605.8	1050	6.86	6.08
		NOSE D (r_n = 0.60 in.)		
30	196.5	1020	6.82	2.10×10^6
31	280.0	1055	6.84	2.81
32	365.4	1035	6.85	3.77
33	436.0	1045	6.86	4.44

TABLE 2.- Concluded

Run number	Stagnation pressure psia	Stagnation temperature ^{o}R	Free-stream Mach number	Free-stream unit Reynolds No. per foot
34	507.6	1040	6.86	5.18
35	604.0	1035	6.86	6.21

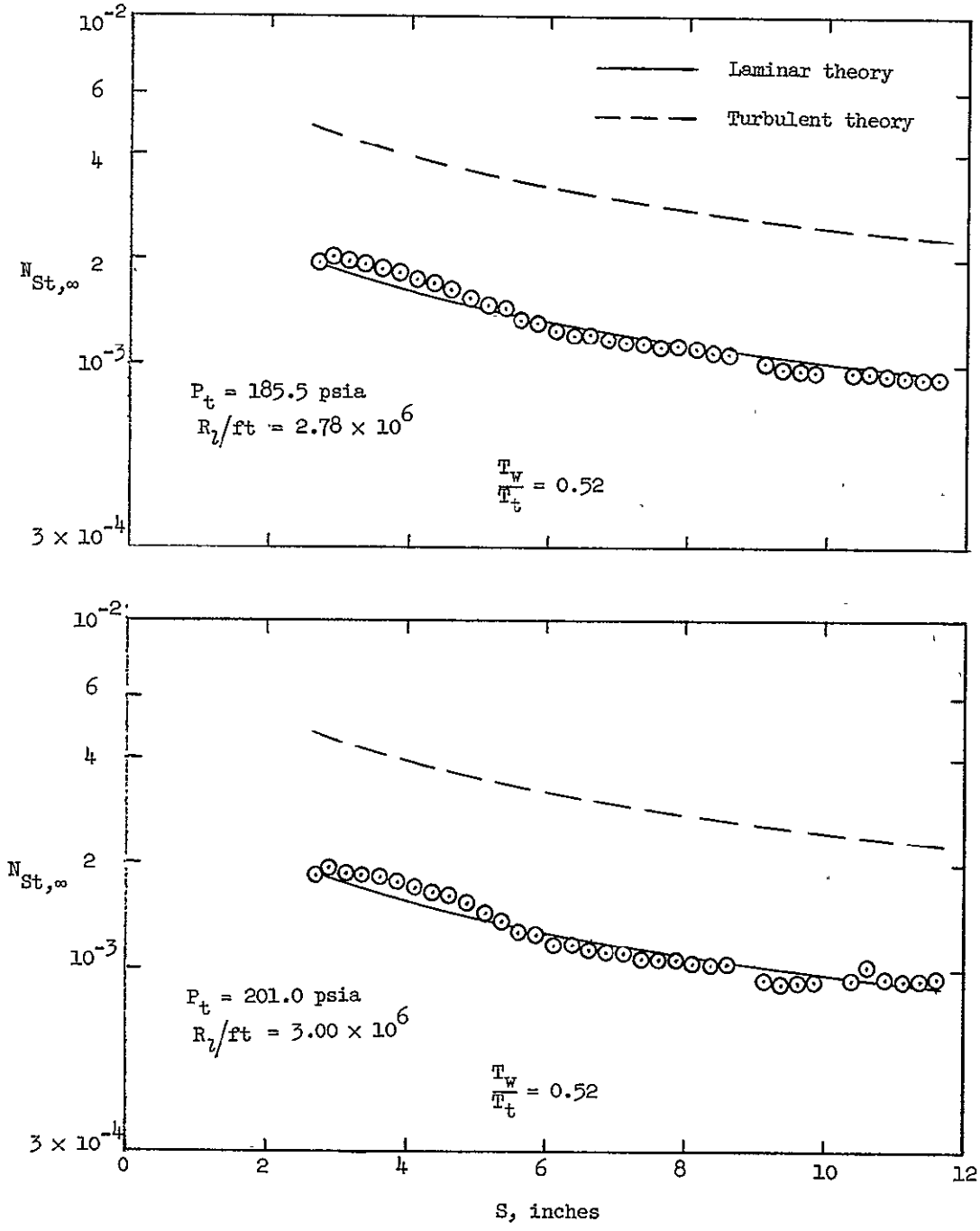

(a) Local unit Reynolds numbers of 2.78 × 10^6 and 3.00 × 10^6 per foot.

Figure 5.- Stanton number distributions for sharp tipped model.

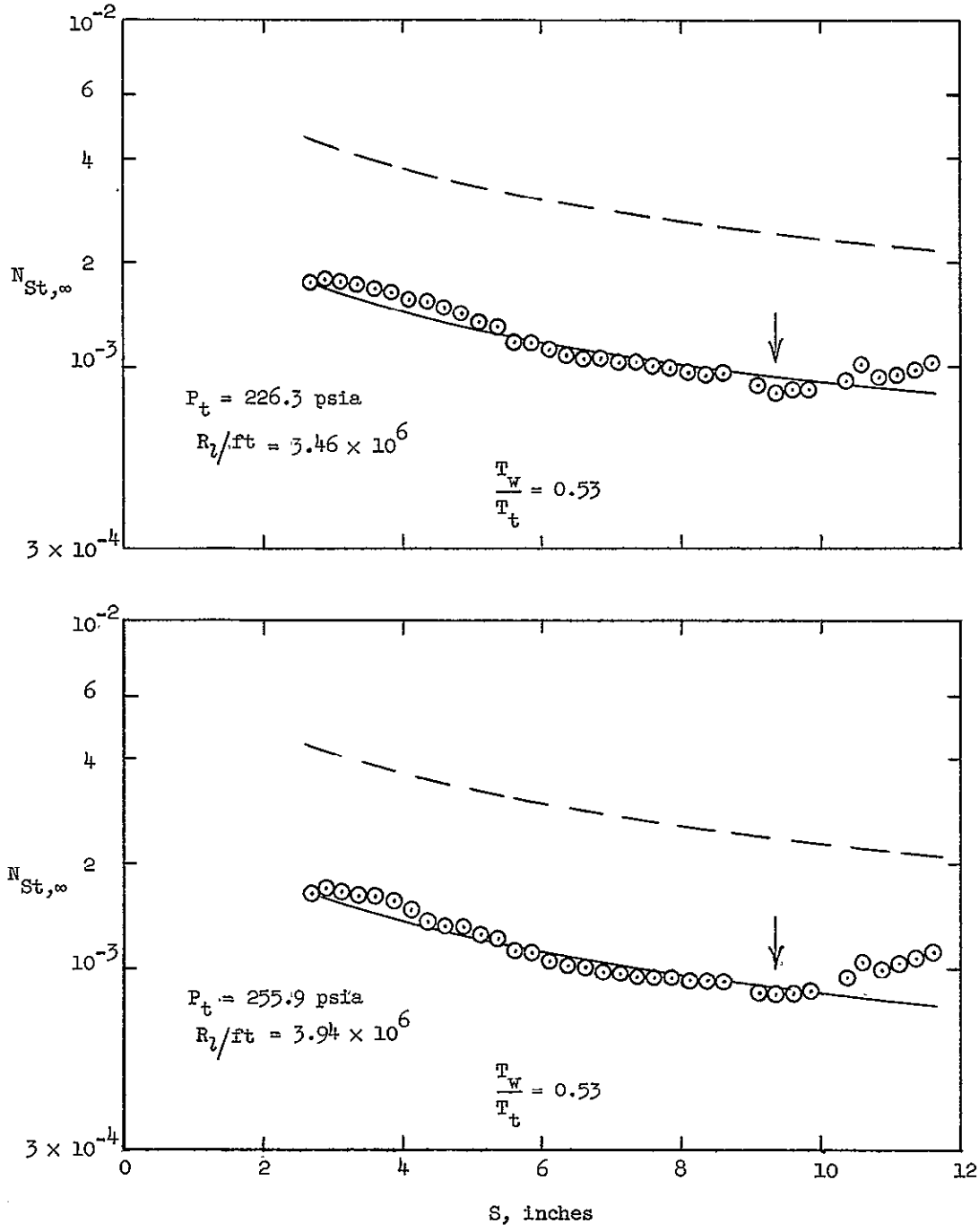

(b) Local unit Reynolds numbers of 3.46×10^6 and 3.94×10^6 per foot.

Figure 5.- Continued.

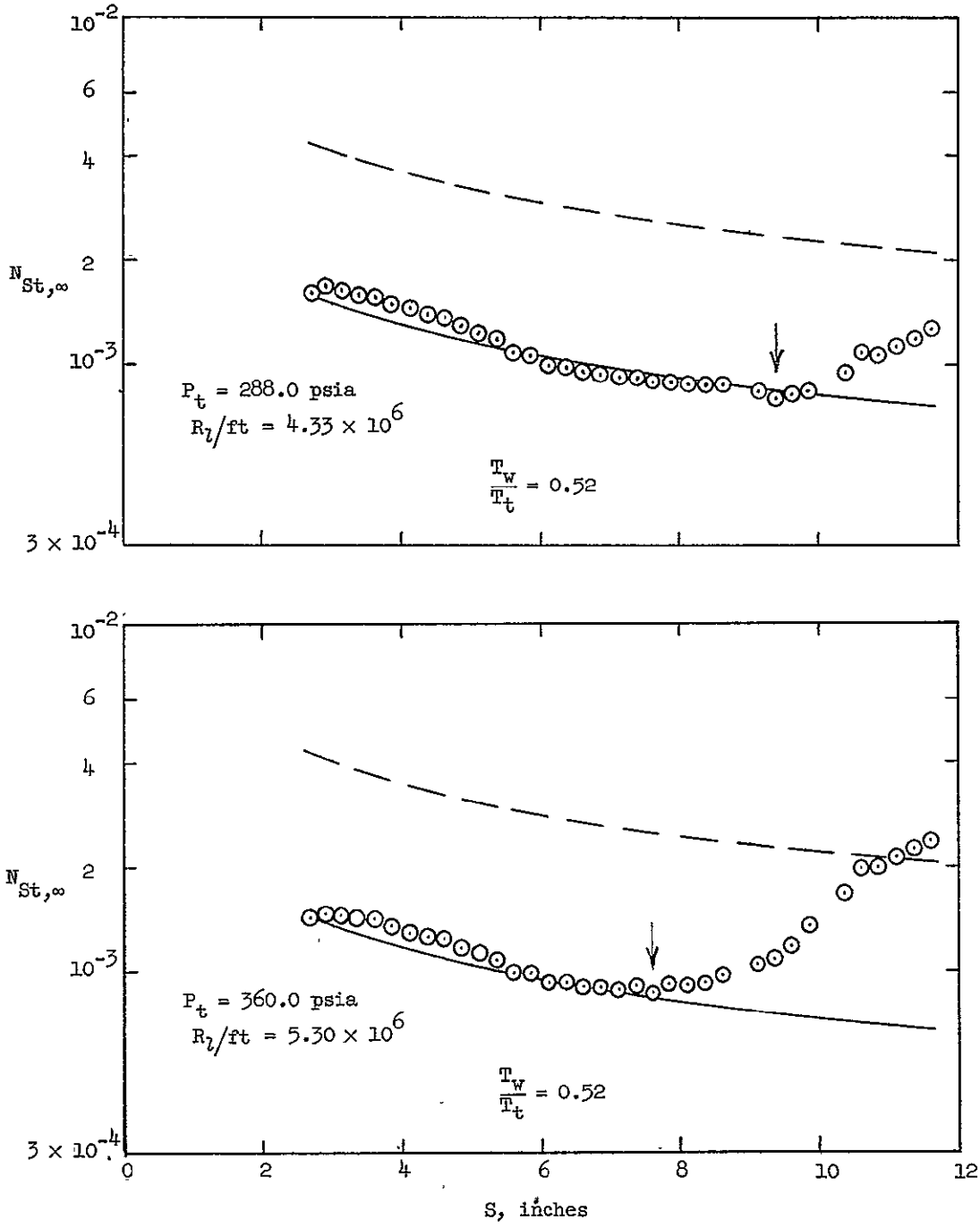

(c) Local unit Reynolds numbers of 4.33×10^6 and 5.30×10^6 per foot.

Figure 5.- Continued.

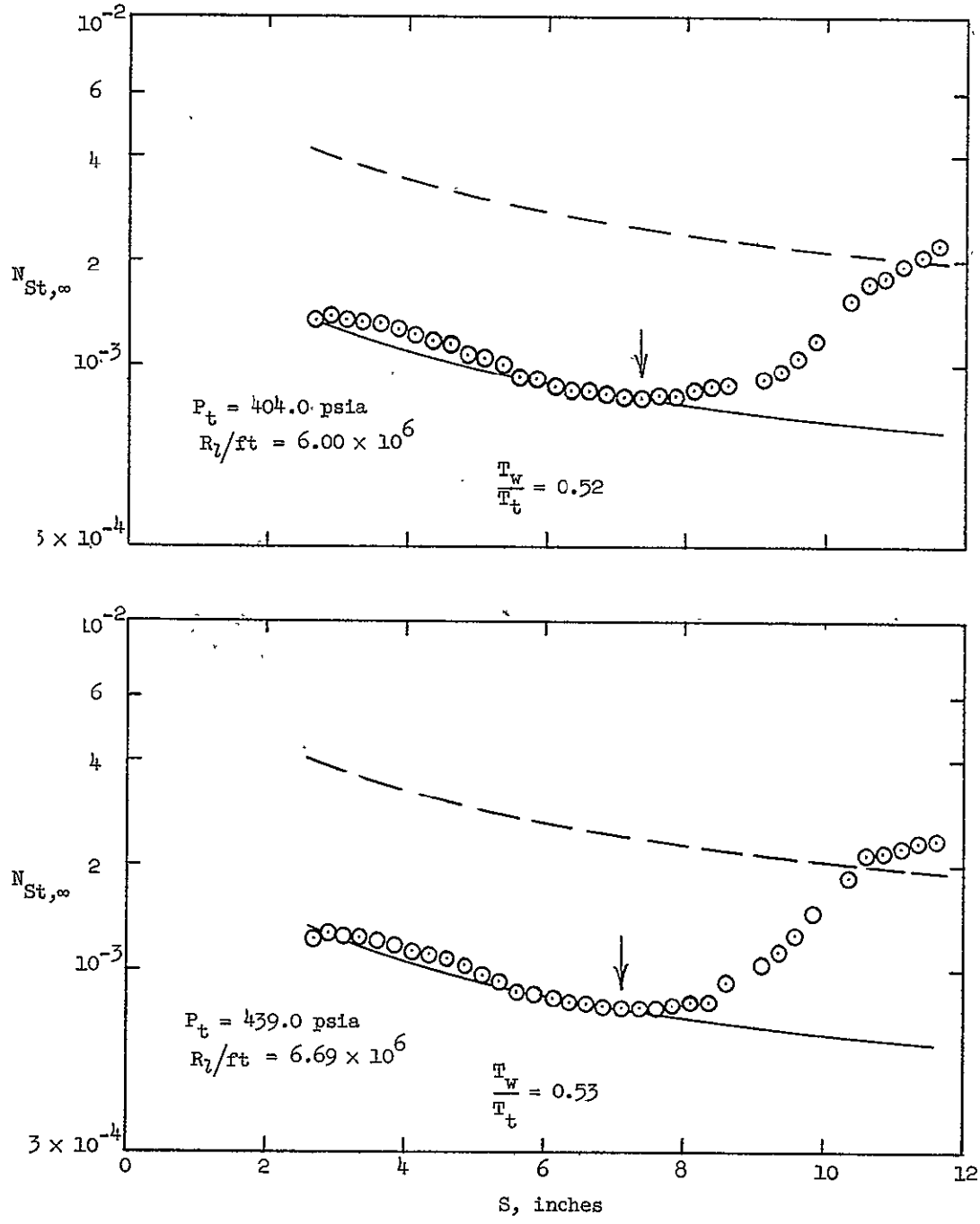

(d) Local unit Reynolds numbers of 6.00×10^6 and 6.69×10^6 per foot.

Figure 5.- Continued.

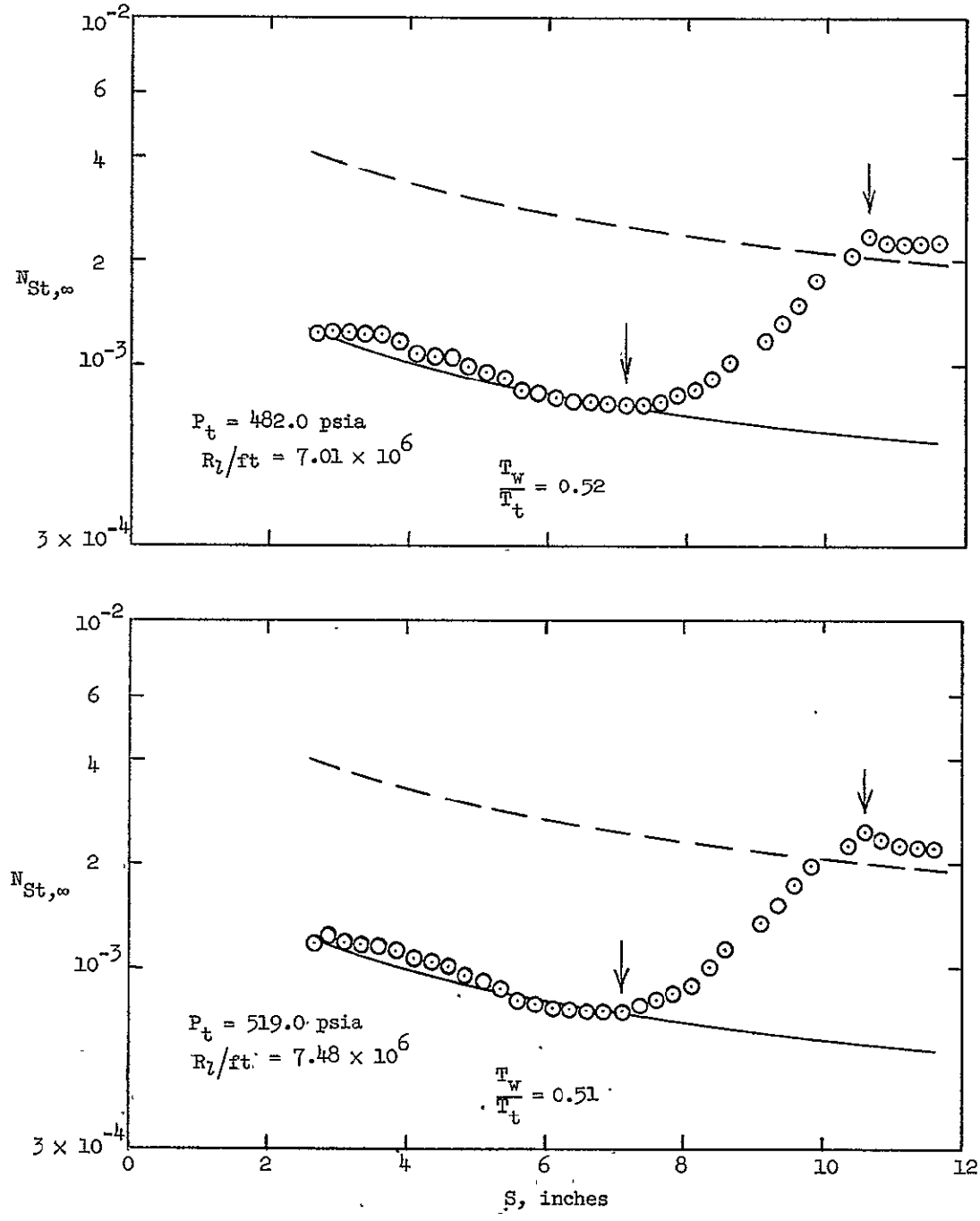

(e) Local unit Reynolds numbers of 7.01×10^6 and 7.48×10^6 per foot.

Figure 5.- Continued.

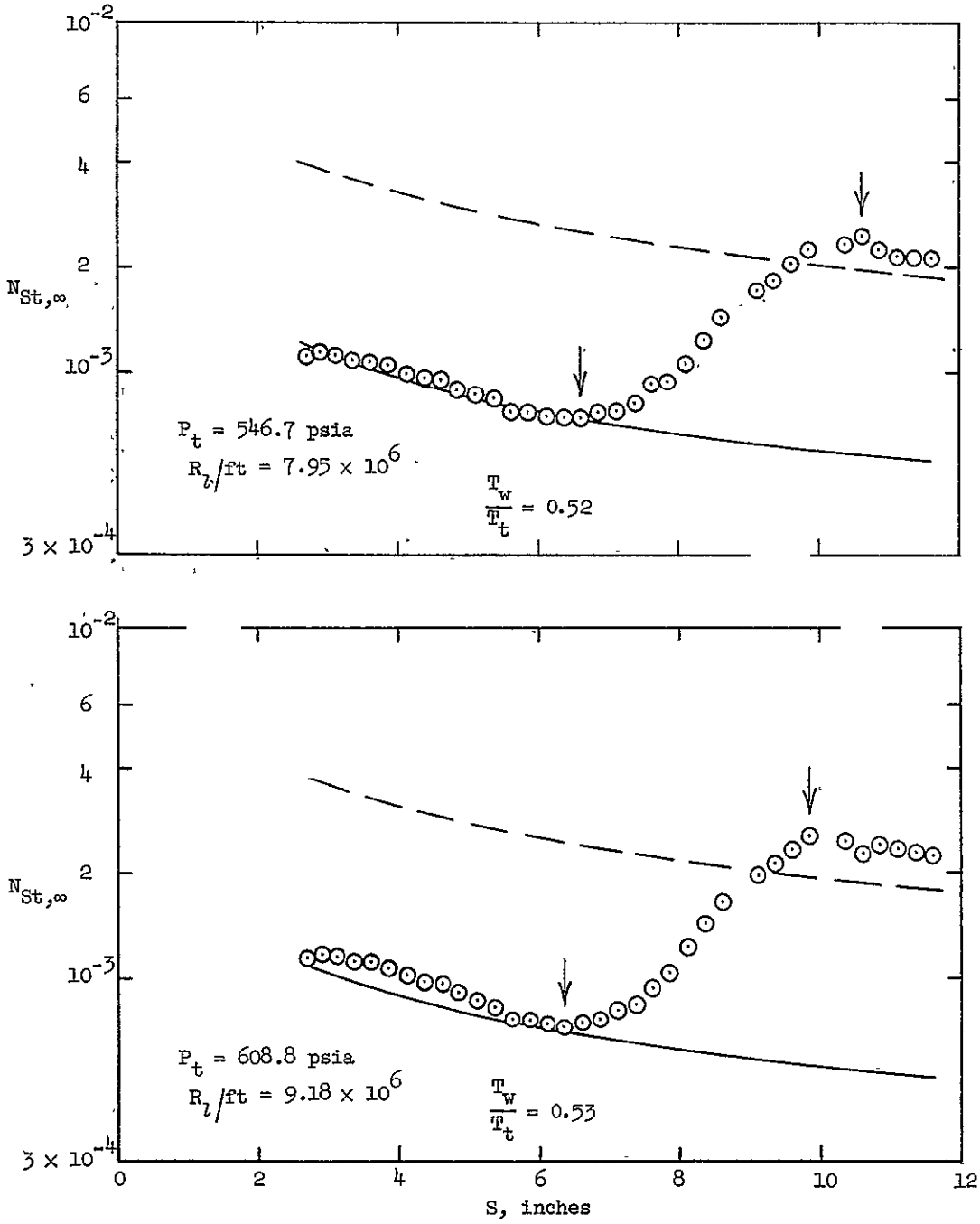

(f) Local unit Reynolds numbers of 7.95×10^6 and 9.18×10^6 per foot.

Figure 5.- Continued.

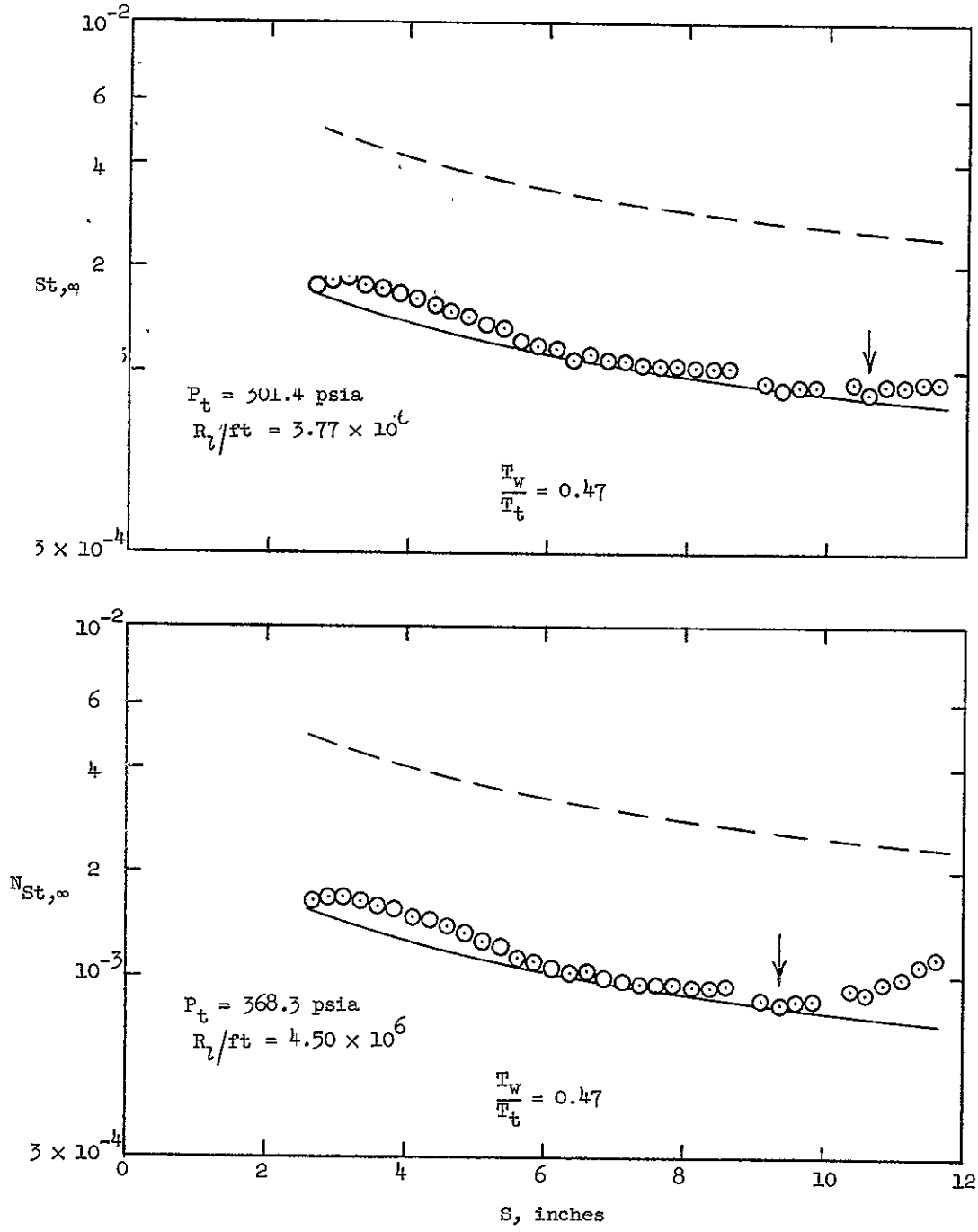

(g) Local unit Reynolds numbers of 3.77×10^6 and 4.50×10^6 per foot.

Figure 5.- Continued.

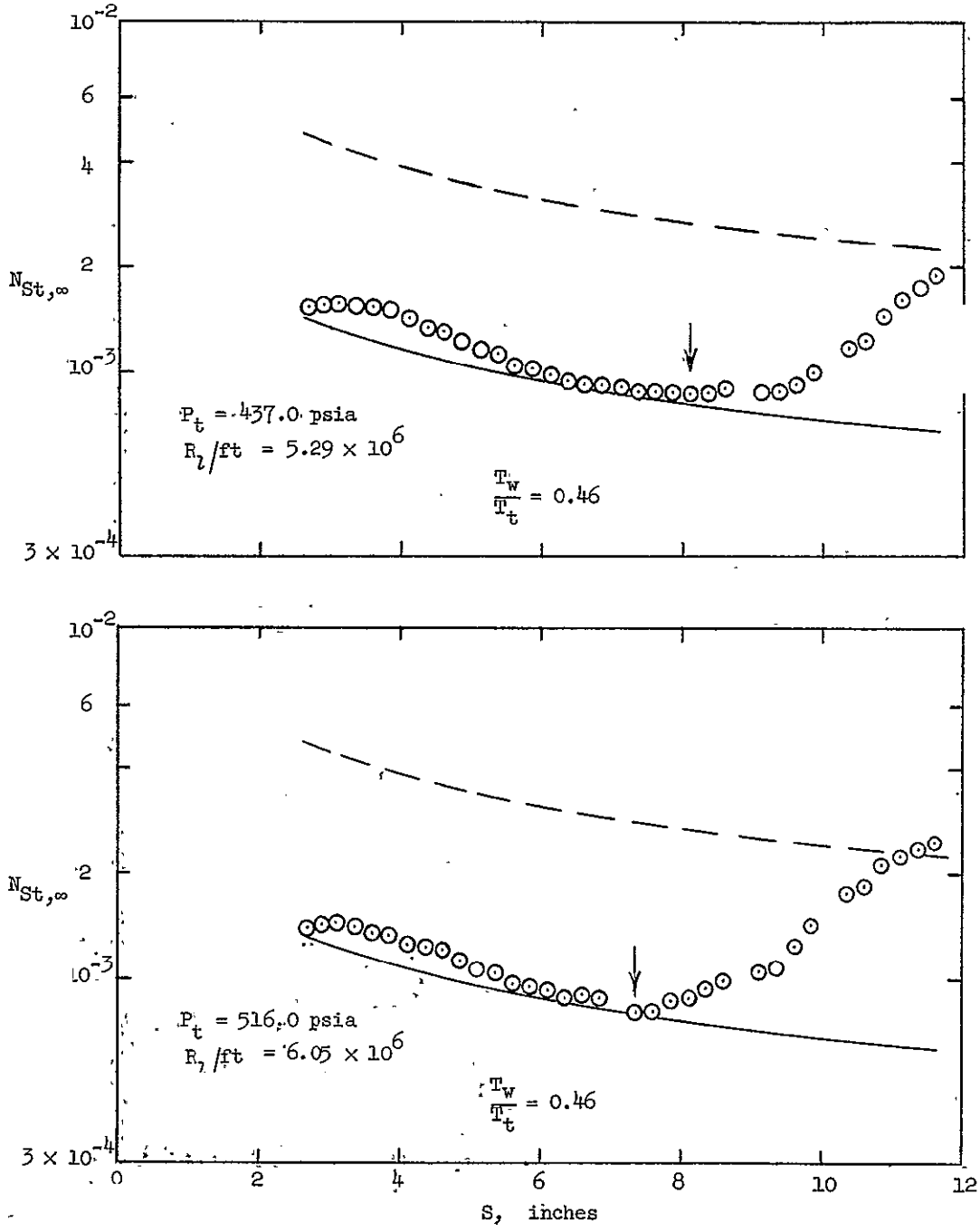

(h) Local unit Reynolds numbers of 5.29×10^6 and 6.05×10^6 per foot.

Figure 5.- Continued.

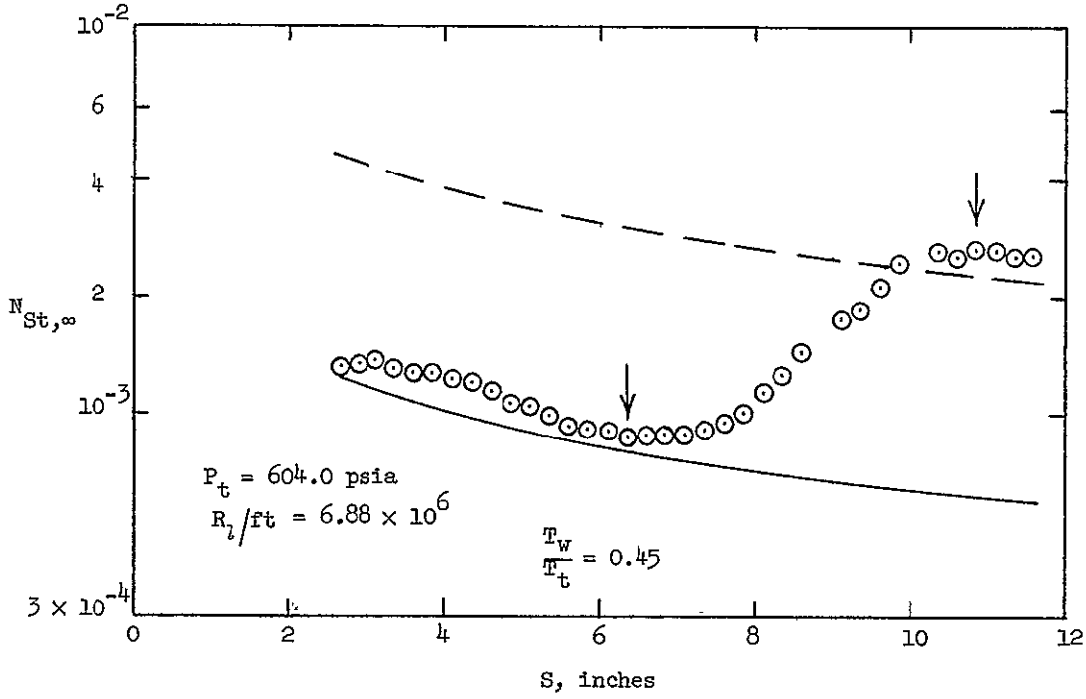

(i) Local unit Reynolds number of 6.88×10^6 per foot.

Figure 5.- Concluded.

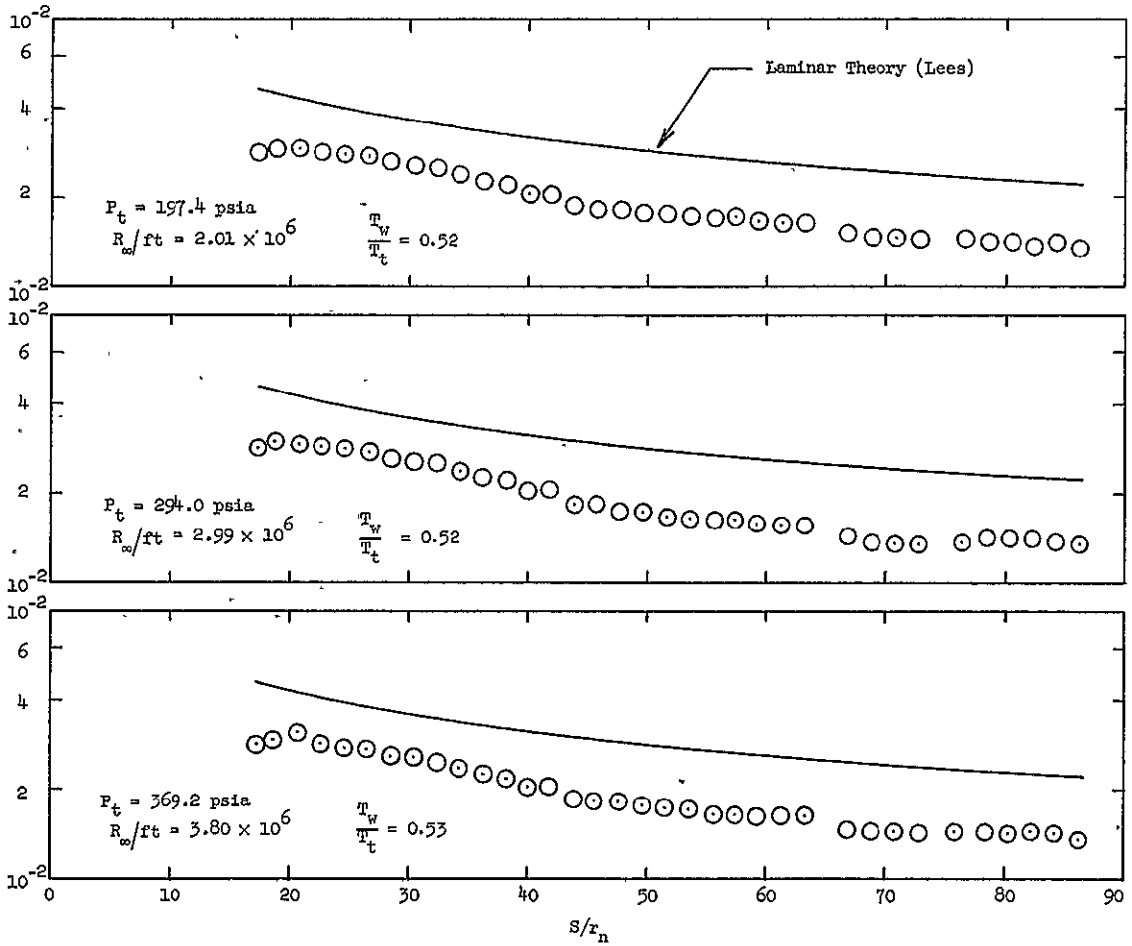

(a) Nose B - free-stream unit Reynolds numbers from 2.01 × 10^6 to 3.80 × 10^6 per foot.

Figure 6.- Wall heat transfer rates for blunt tipped model nondimensionalized by nose stagnation heating rates.

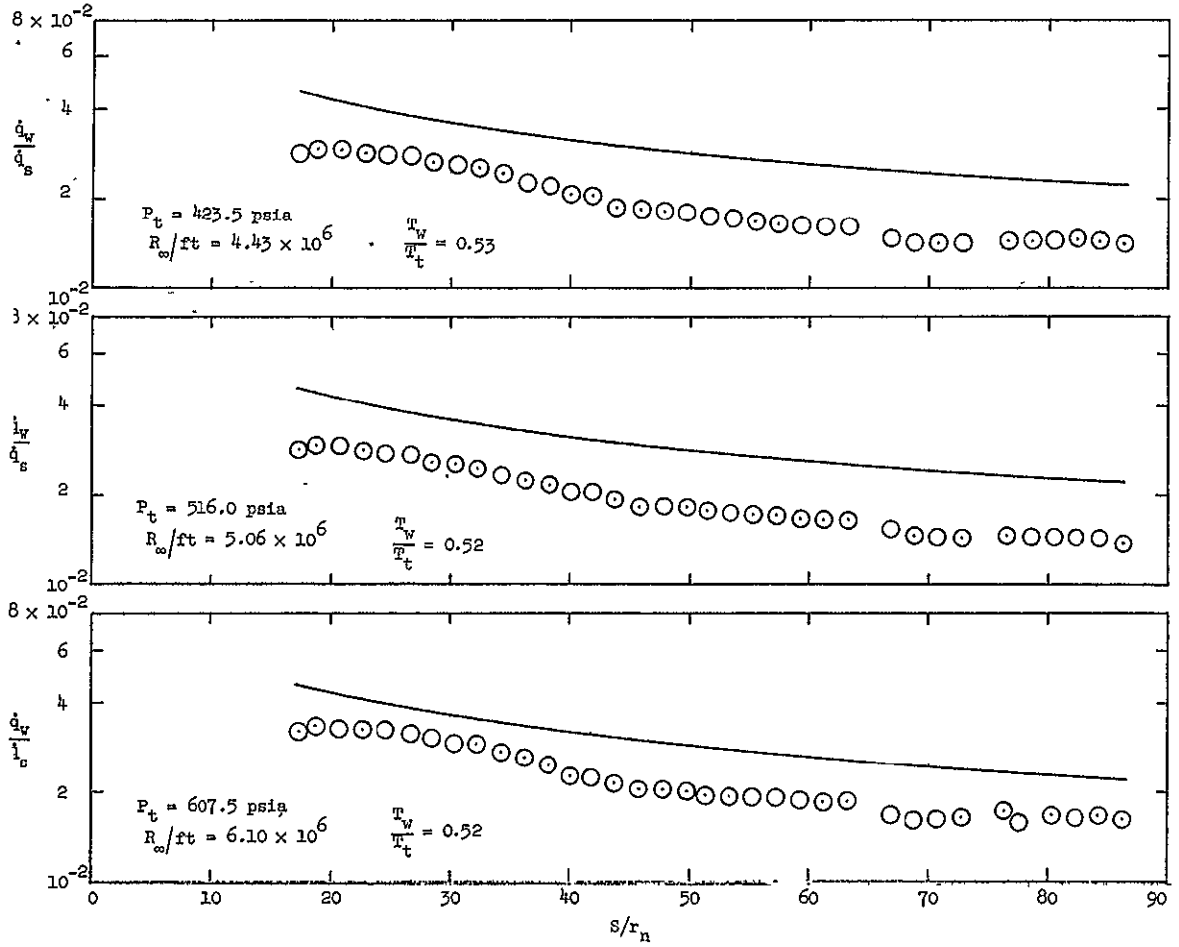

(b) Nose B - free-stream unit Reynolds numbers from 4.43×10^6 to 6.10×10^6 per foot.

Figure 6.- Continued.

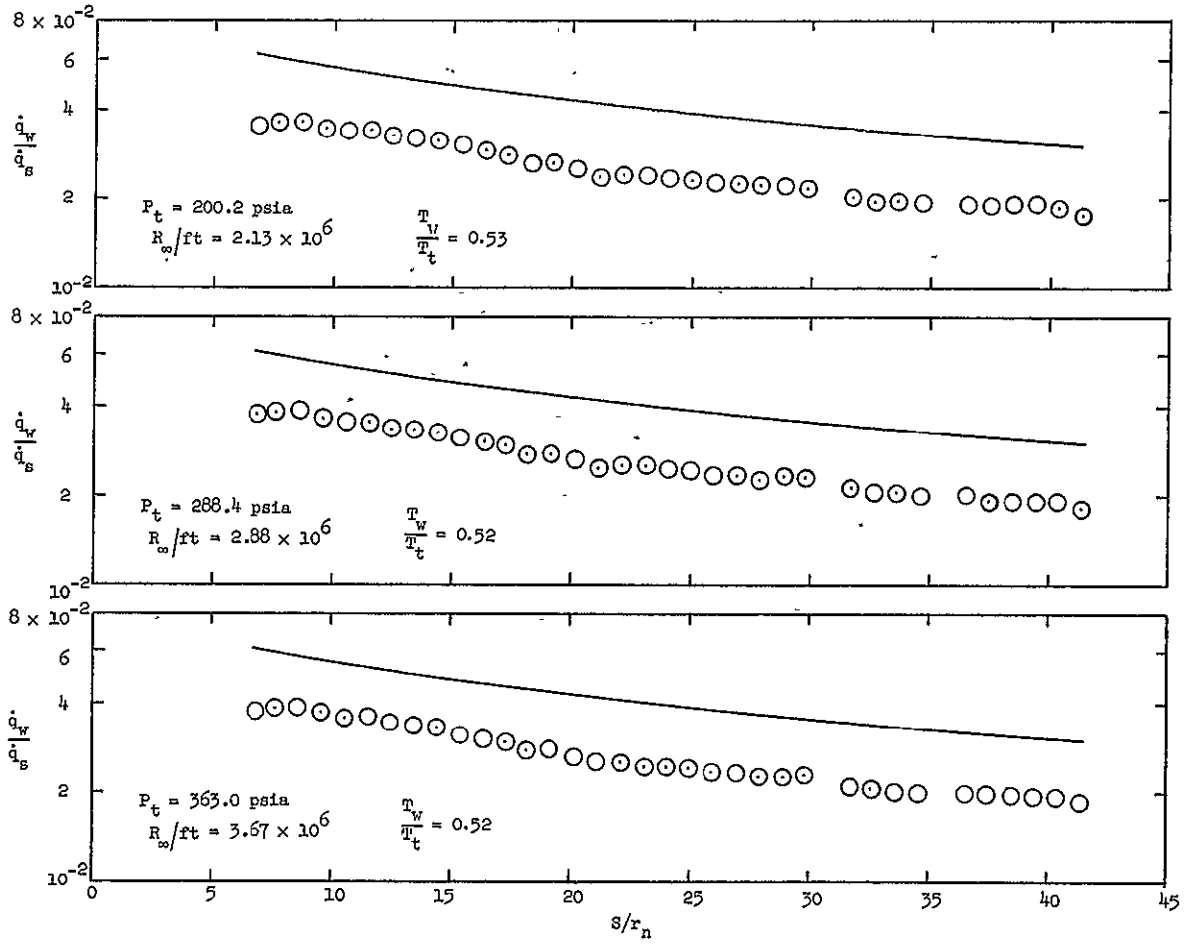

(c) Nose C - free-stream unit Reynolds numbers from 2.13×10^6 to 3.67×10^6 per foot.

Figure 6.- Continued.

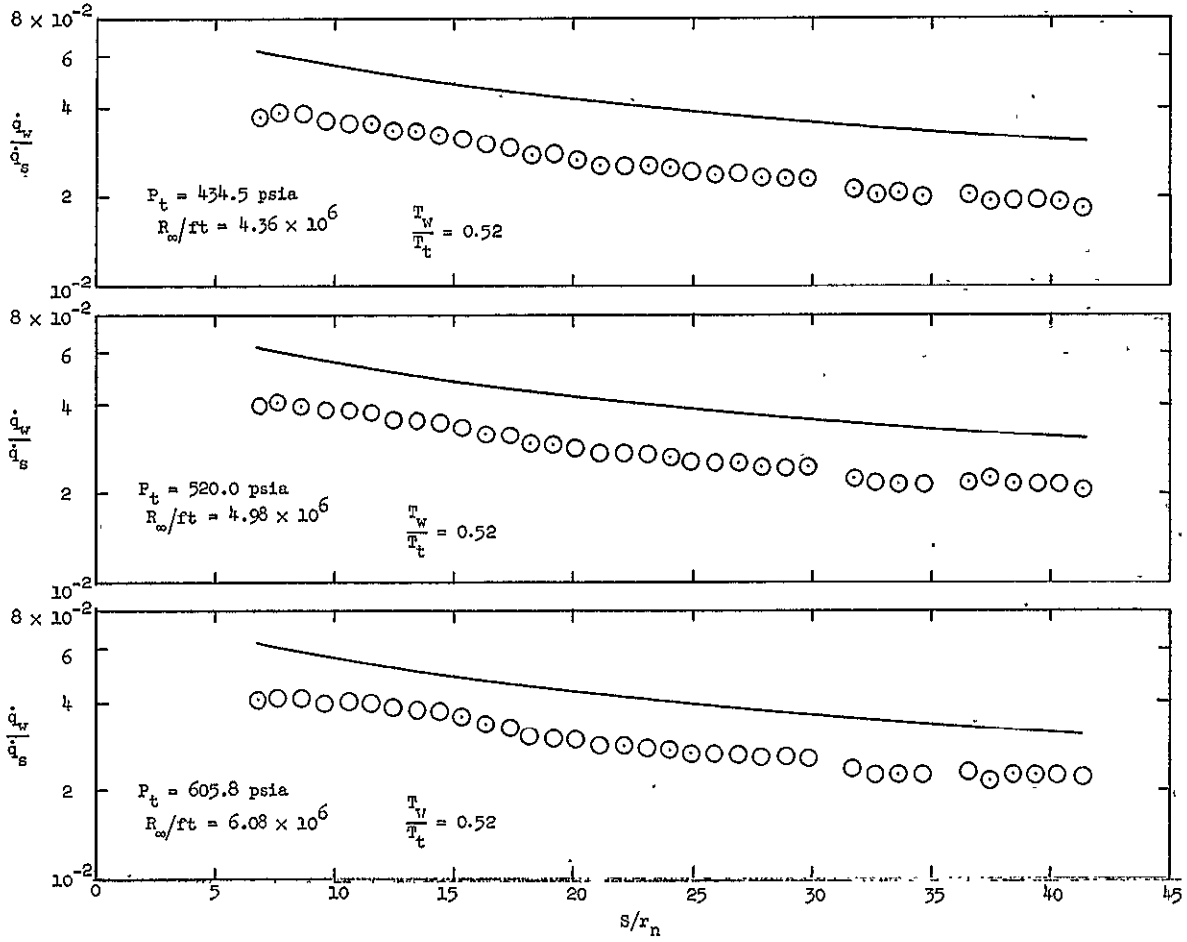

(d) Nose C - free-stream unit Reynolds numbers from 4.36×10^6 to 6.08×10^6 per foot.

Figure 6.- Continued.

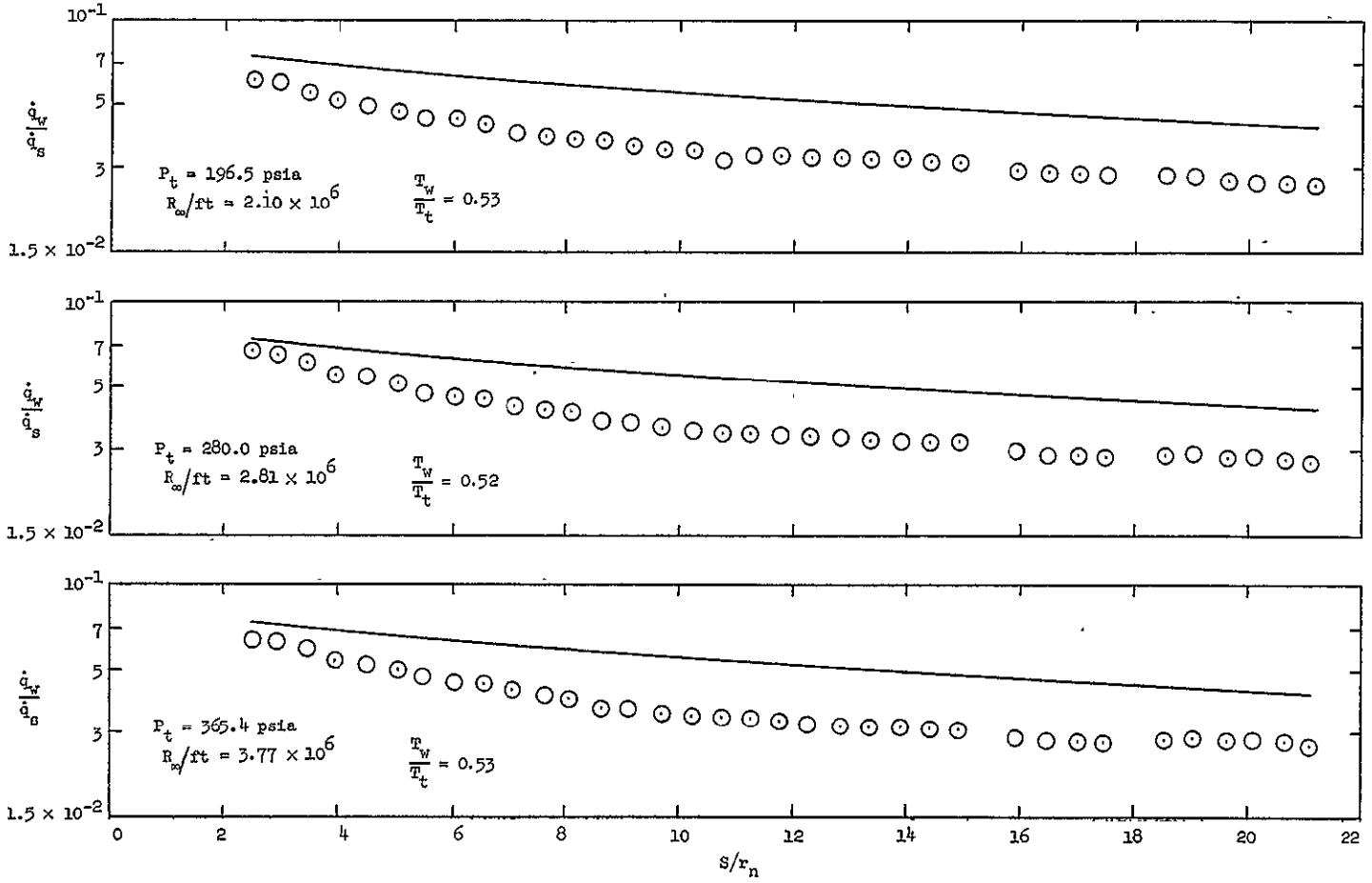

(e) Nose D - free-stream unit Reynolds numbers from 2.10×10^6 to 3.77×10^6 per foot.

Figure 6.- Continued.

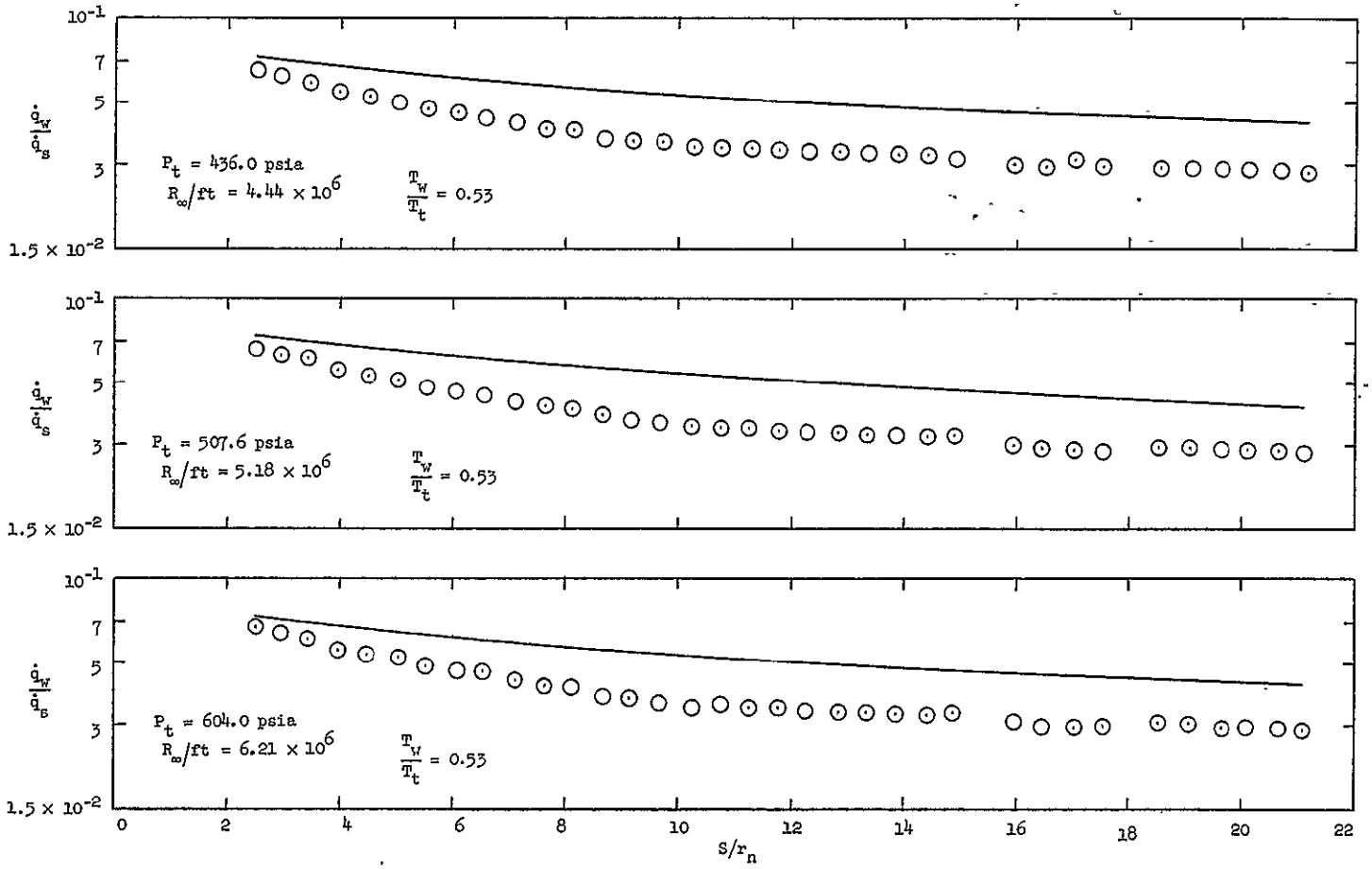

(f) Nose D - free-stream unit Reynolds numbers from 4.44×10^6 to 6.21×10^6 per foot.

Figure 6.- Concluded.

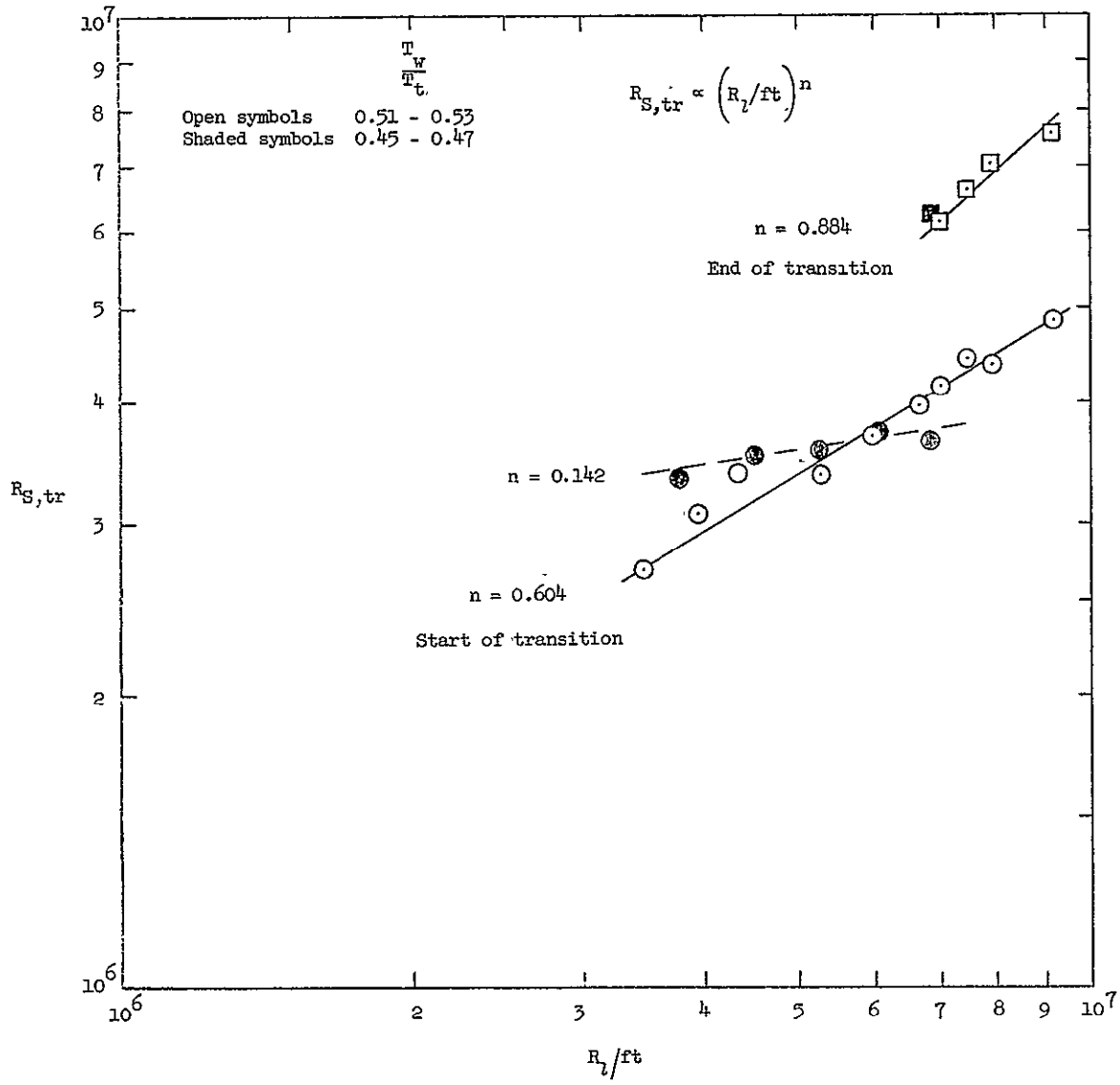

Figure 7.- Effect of local unit Reynolds number on transition Reynolds number for sharp cone.

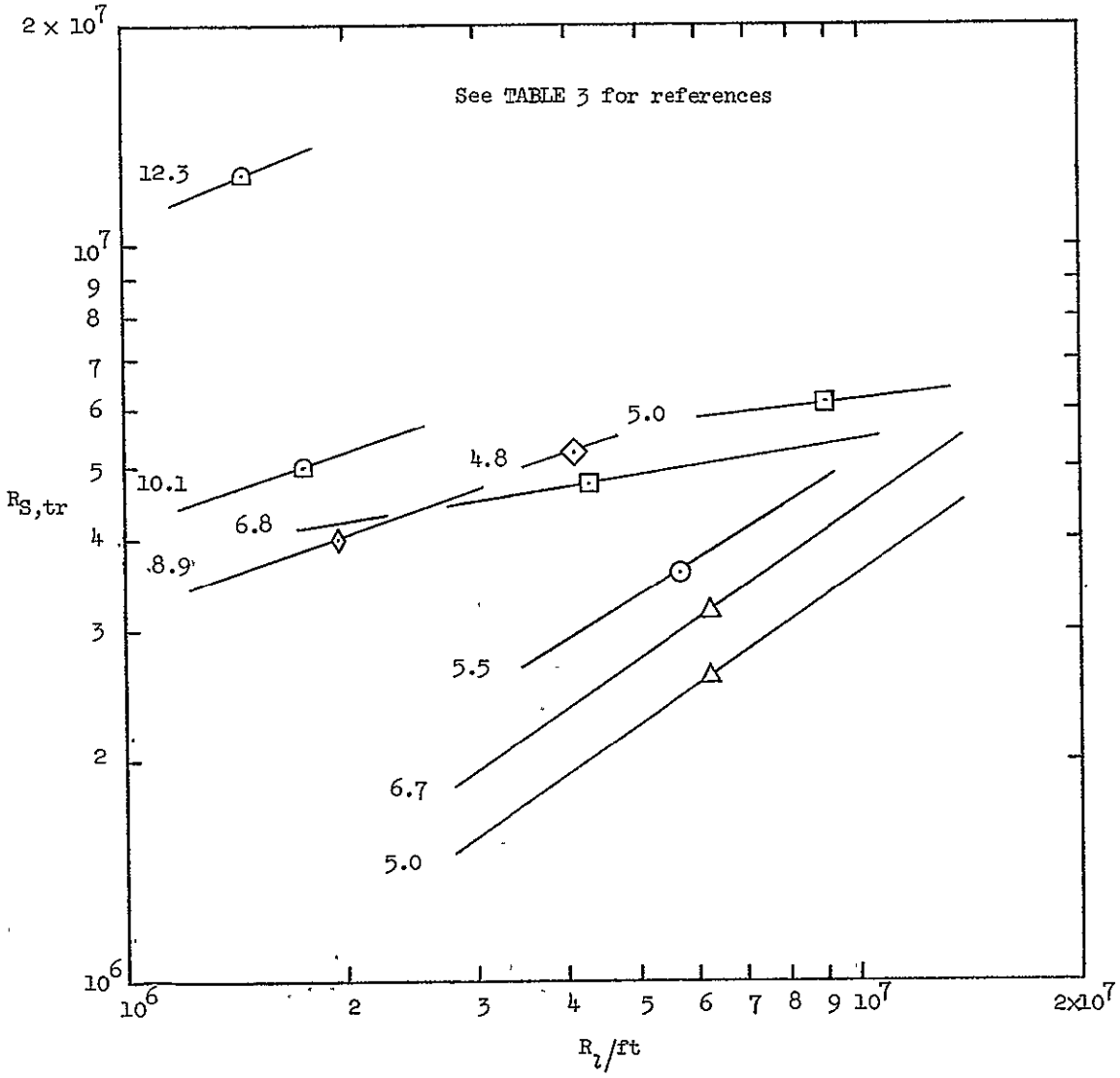

Figure 8.- Effect of local unit Reynolds number on transition Reynolds number for slender sharp cones from various facilities.

TABLE 3.- LIST OF REFERENCES FOR TRANSITION DATA ON SHARP CONES

SYMBOL	M_l	θ_c (deg.)	T_w/T_t	$\rho_l u_l/\mu_l$	Investigator
⊙	5.5	10	.45-.53	3.5×10^6-9.2×10^6	Present
⊡	5.0	15	.43	6×10^6-13.5×10^6	Larson and Mateer (ref. 6)
	6.8	5	.43	1.7×10^6-10.7×10^6	
◈	4.8	8	.38-.45	3.5×10^6-4.7×10^6	Stetson and Rushton (ref. 1)
△	5.0	15.8	.43	2.8×10^6-13.8×10^6	Stainback (ref. 2)
	6.7	7.5	.43	2.8×10^6-13.8×10^6	
	7.3	5	.43	1.5×10^6-10.0×10^6	
◺	8.8	5	.075-.365	2×10^6	Sanator, et al (ref. 3)
◈	8.9	3.75	.55-.69	1.3×10^6-3.1×10^6	Everhart and Hamilton (ref. 23)
⊡	10.1	5	.21-.26	1.2×10^6-2.6×10^6	Softley, et al (ref. 4)
	12.3	5	.21-.25	1.2×10^6-1.8×10^6	

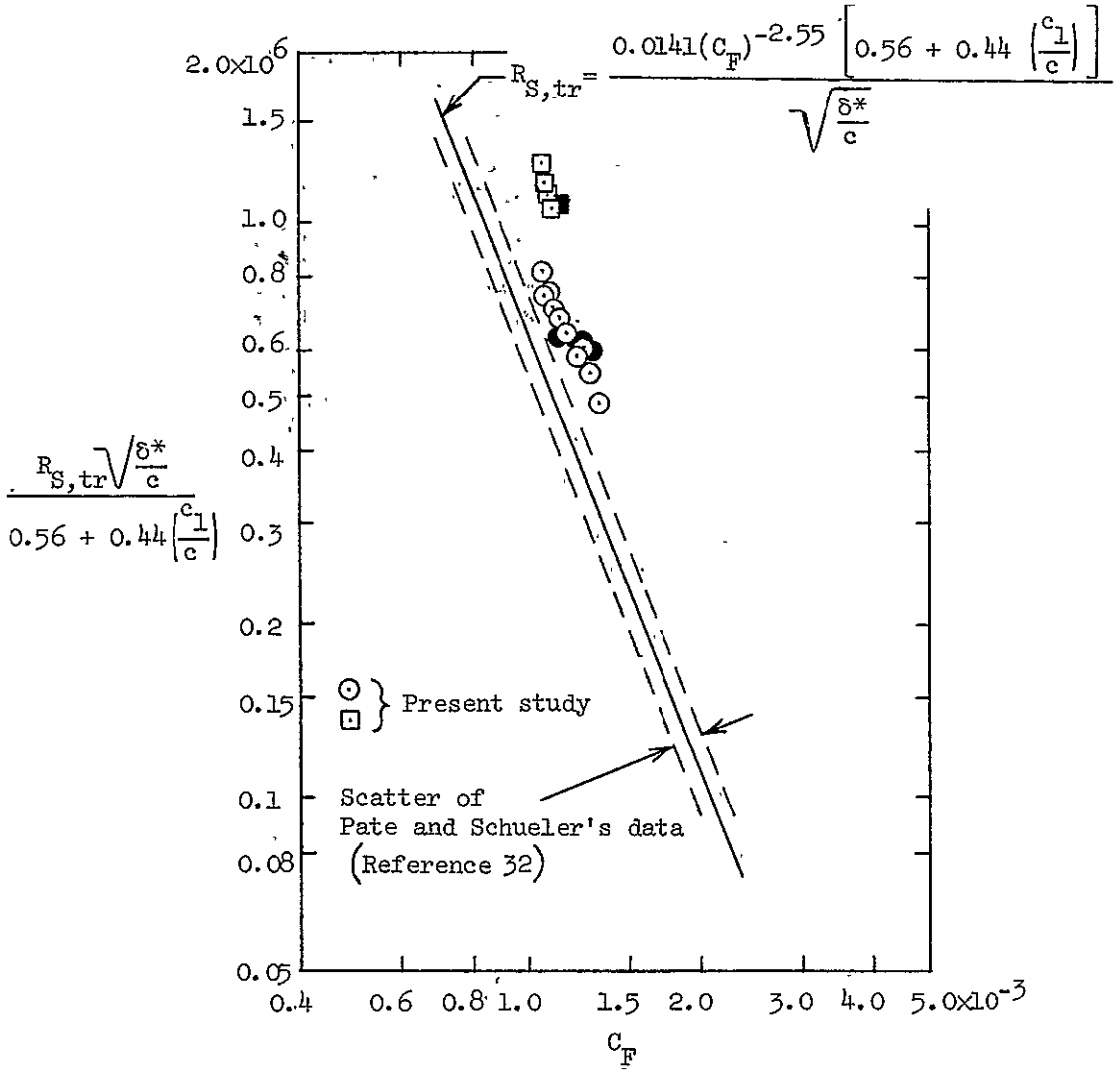

Figure 9.- Comparison of present transition data with Pate and Schueler's correlation.

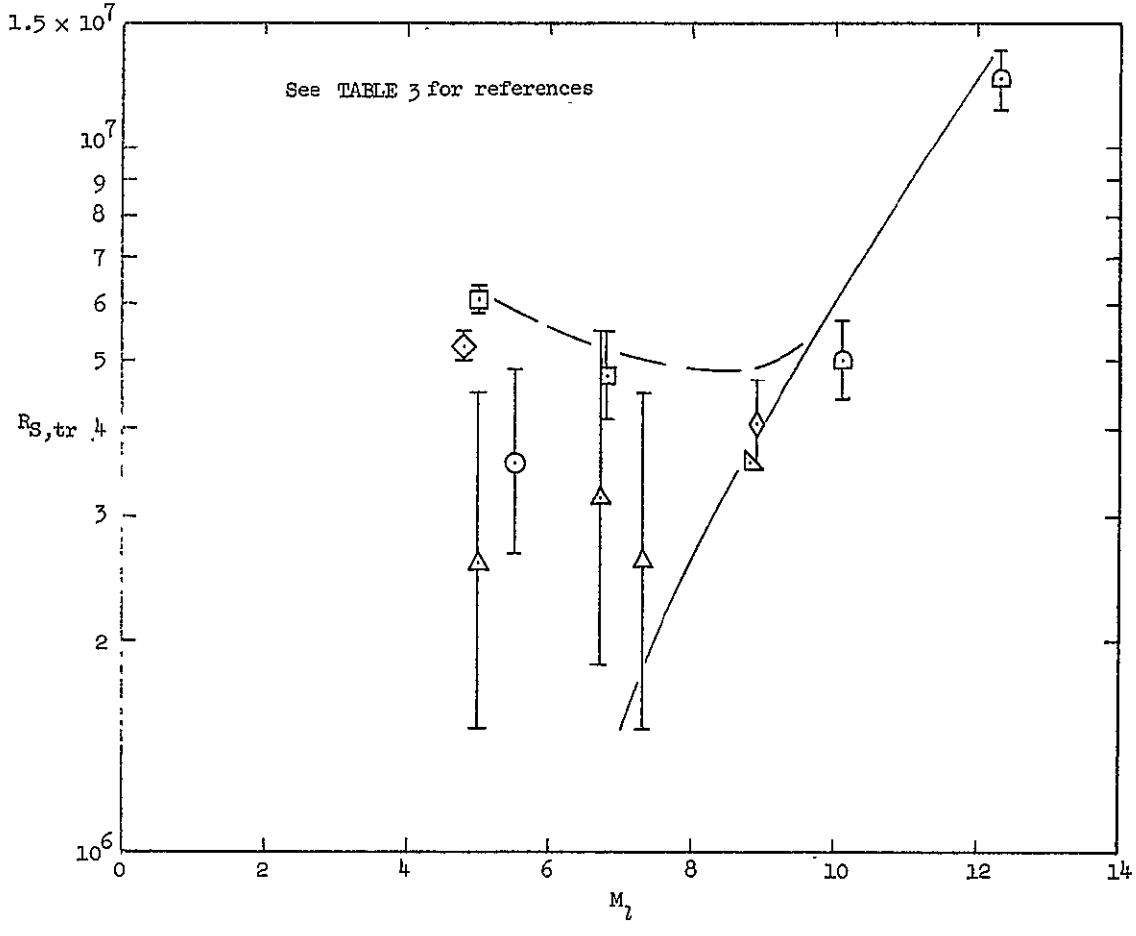

(a) Variable local unit Reynolds number.

Figure 10.- Effect of local Mach number on transition Reynolds number for slender sharp cones from various facilities.

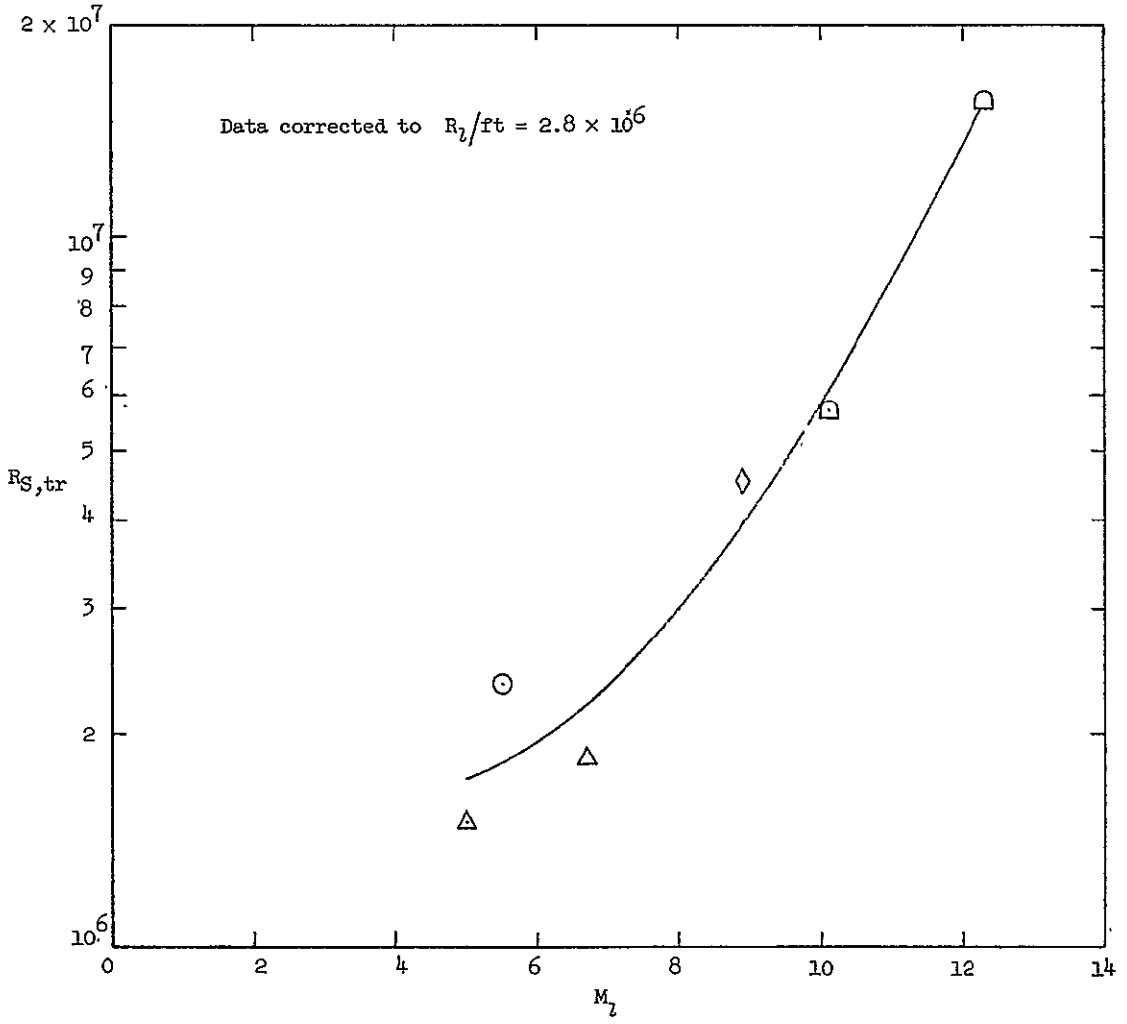

(b) Local unit Reynolds number = 2.8×10^6 per foot.

Figure 10.- Continued.

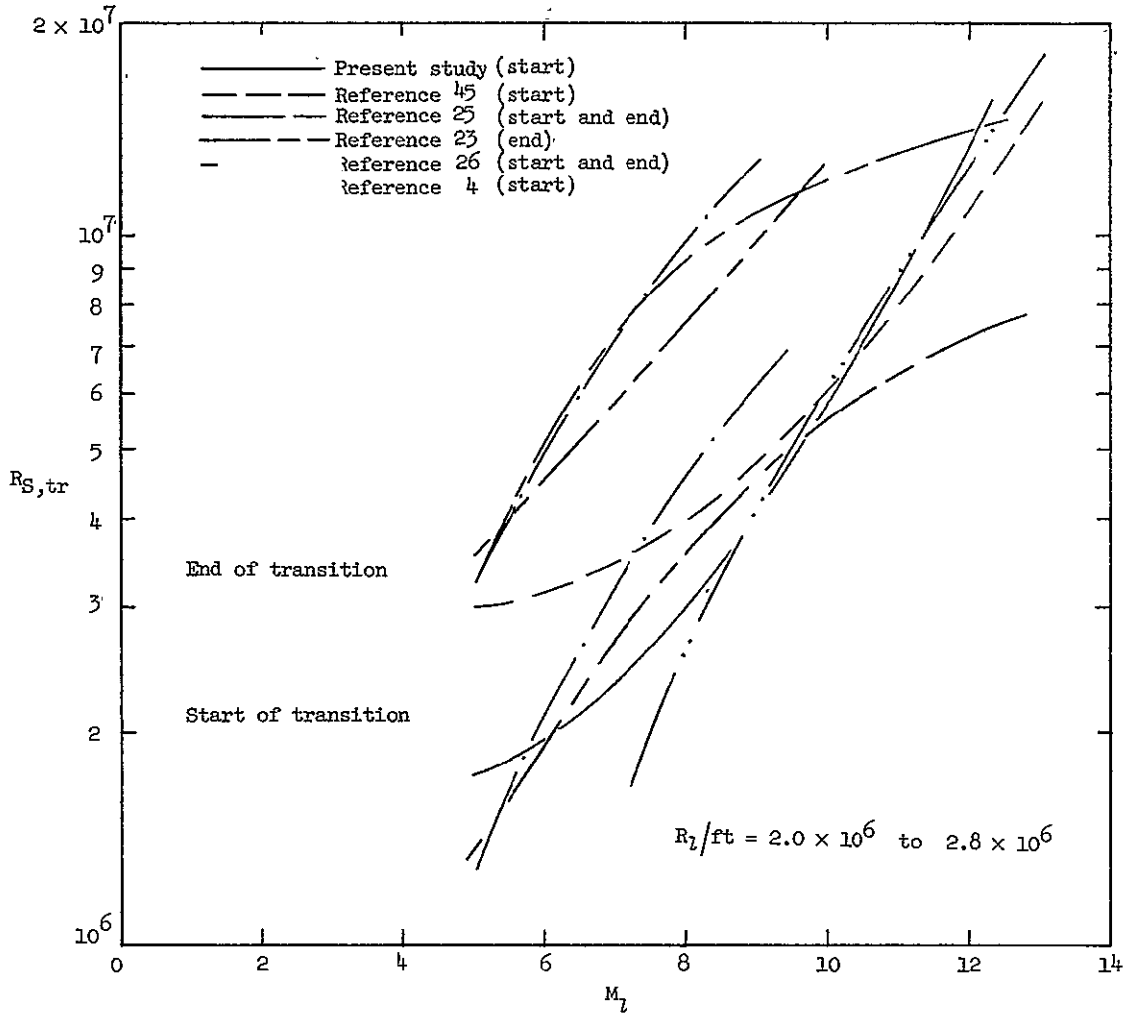

(c) Correlations from various investigations.

Figure 10.- Concluded.

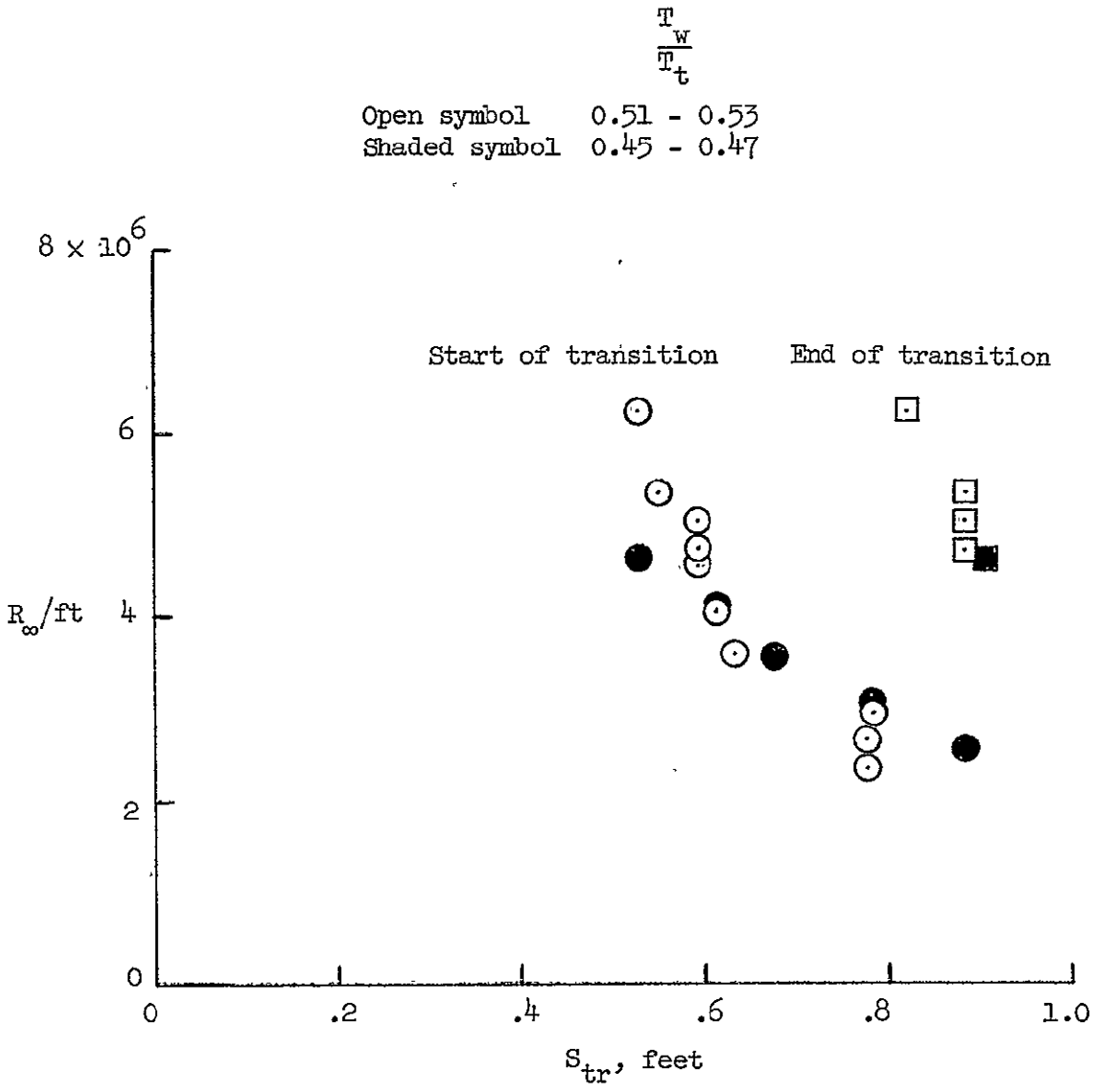

Figure 11.- Effect of free-stream unit Reynolds number on transition location.

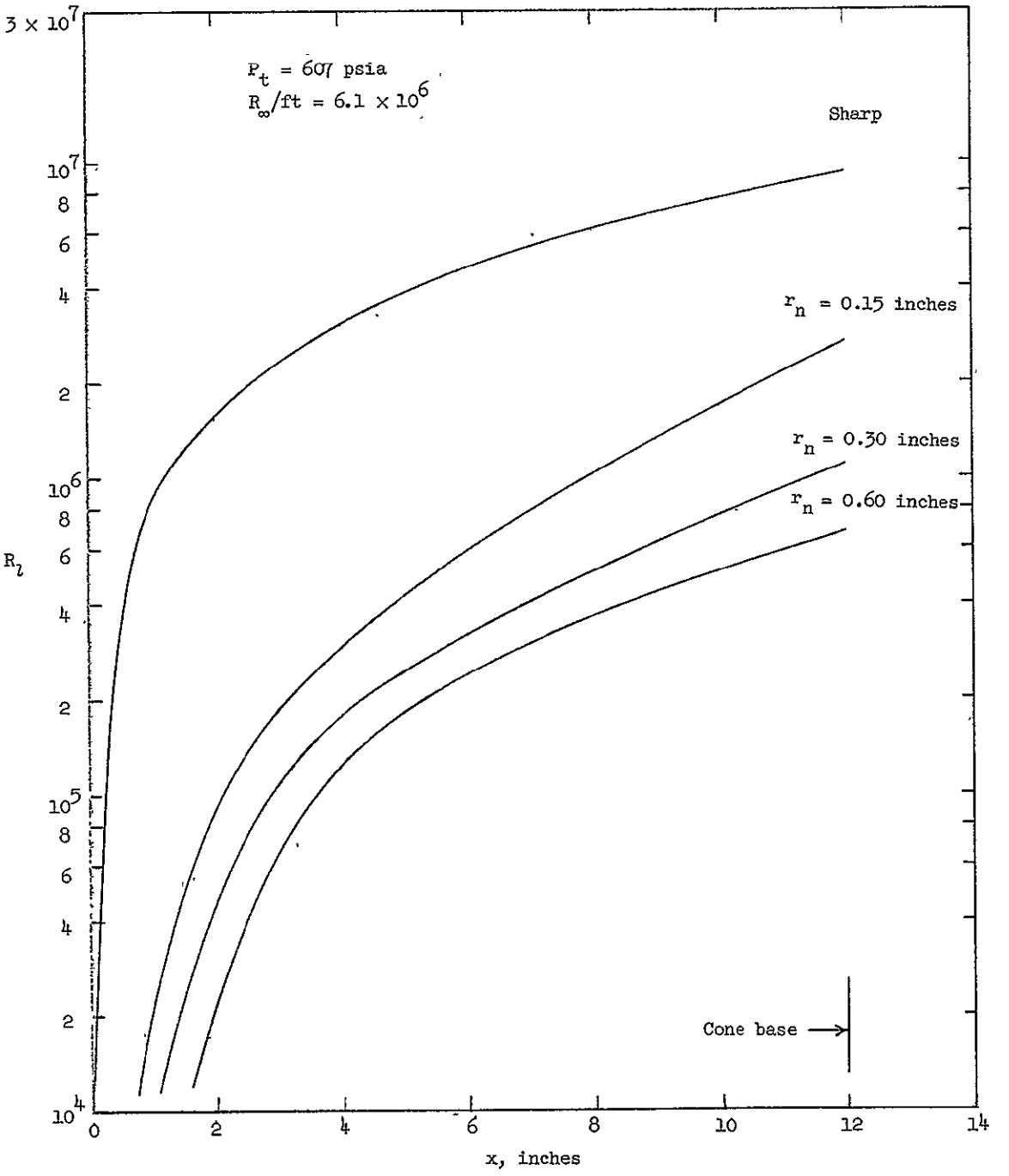

Figure 12.- Local Reynolds number distribution for sharp and blunt tipped cone.

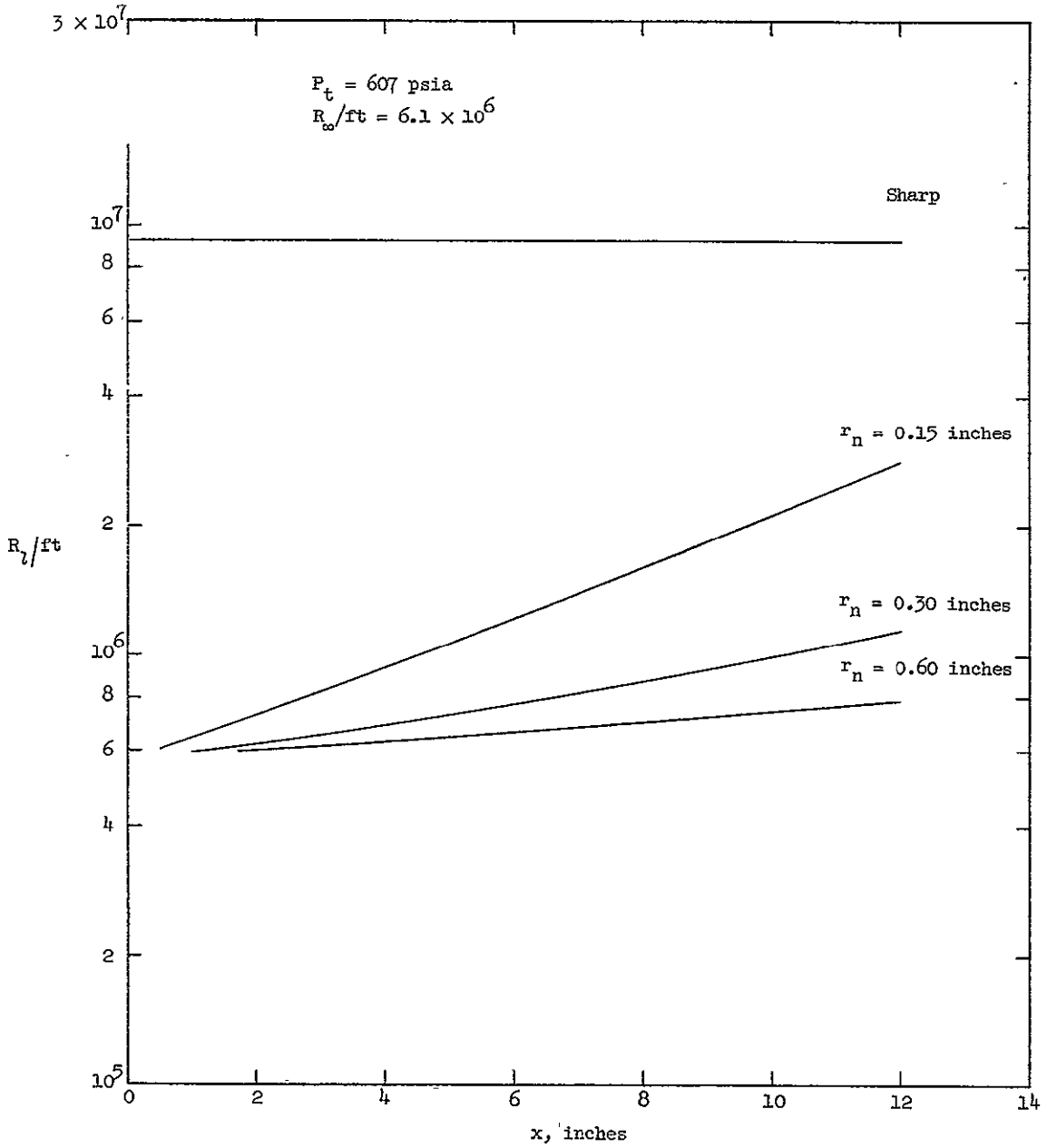

Figure 13.- Local unit Reynolds number distribution for sharp and blunt tipped cone.

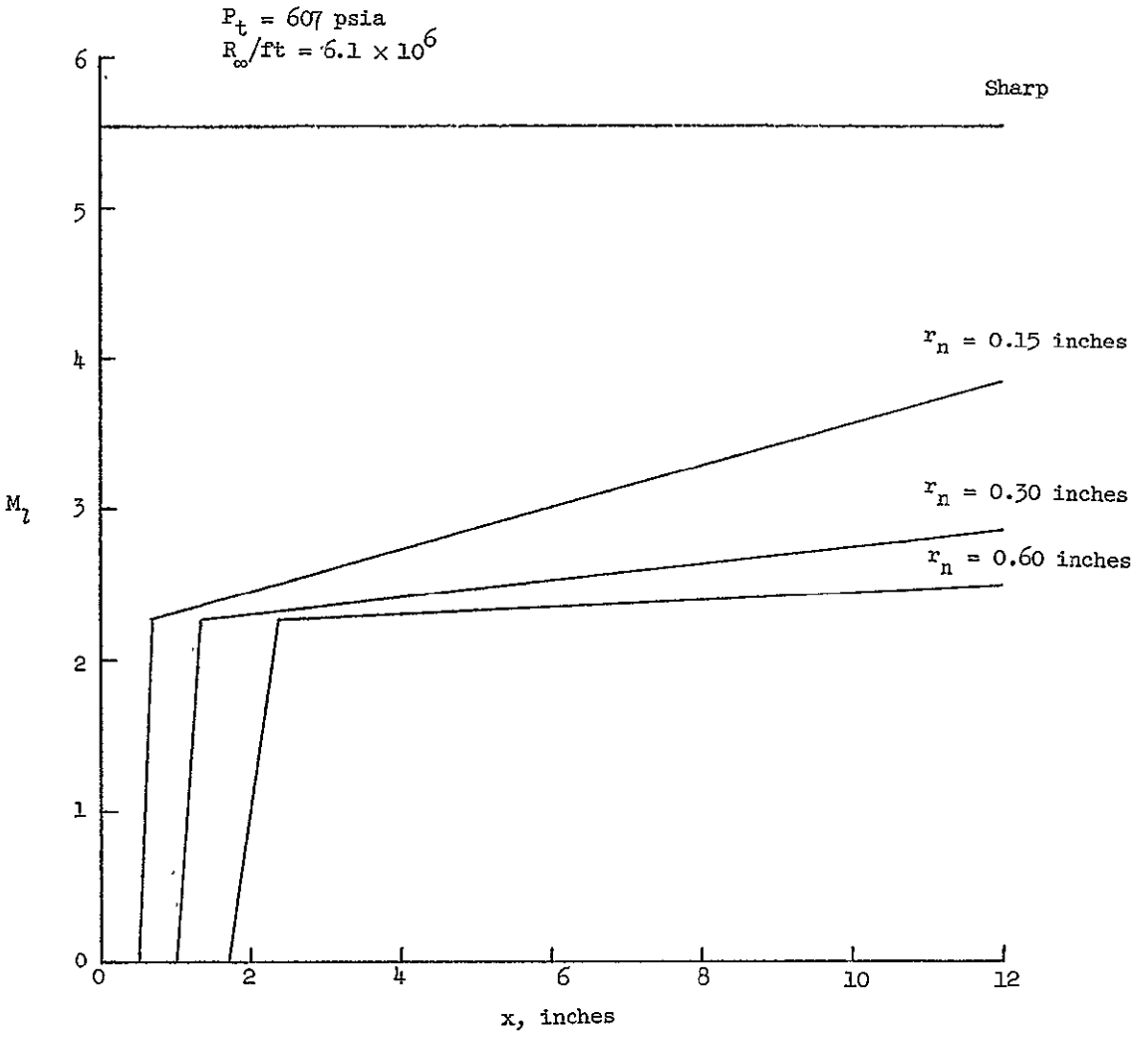

Figure 14.- Local Mach number distribution for sharp and blunt tipped cone.

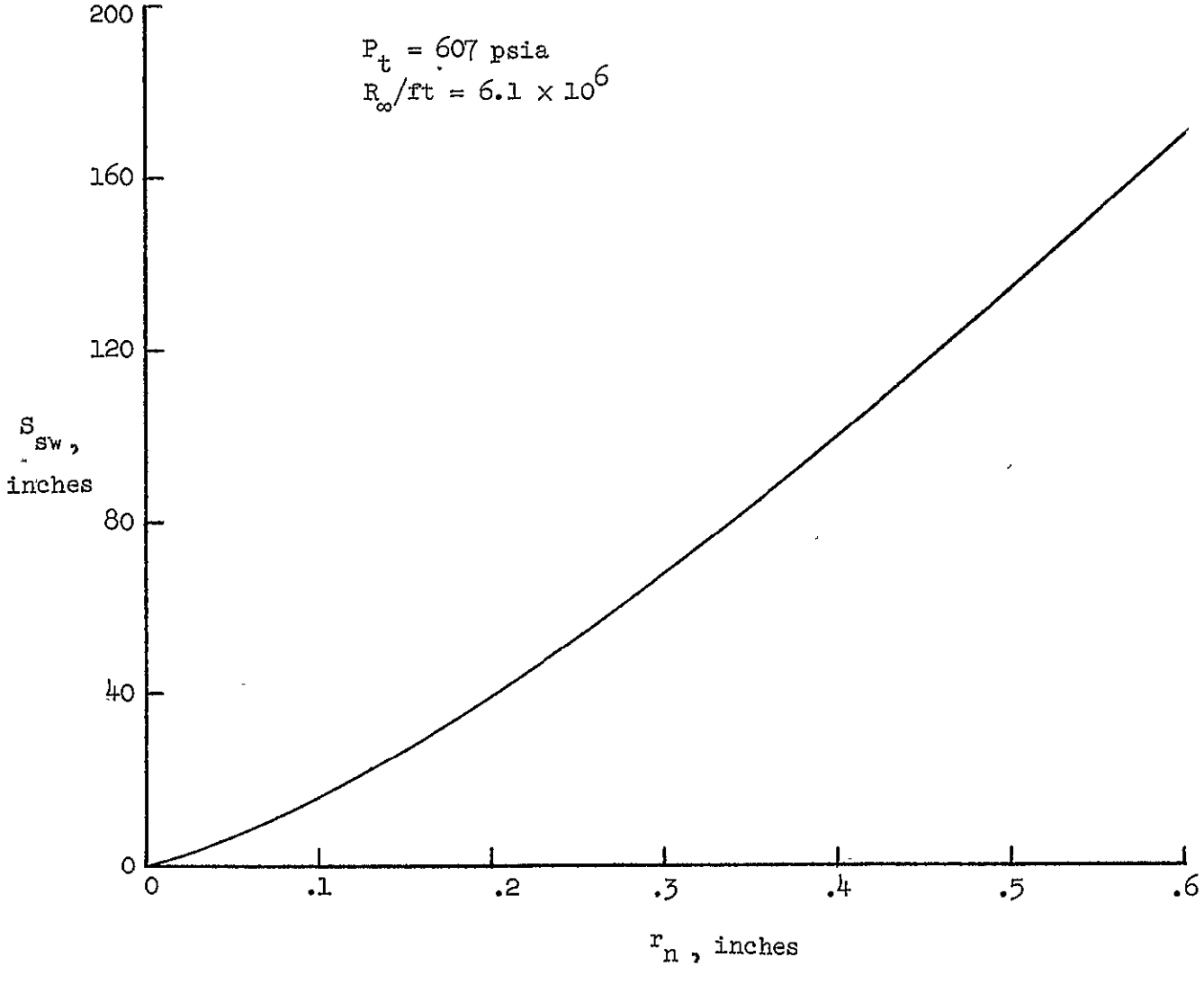

Figure 15.- Variation of swallowing distance with nose bluntness.

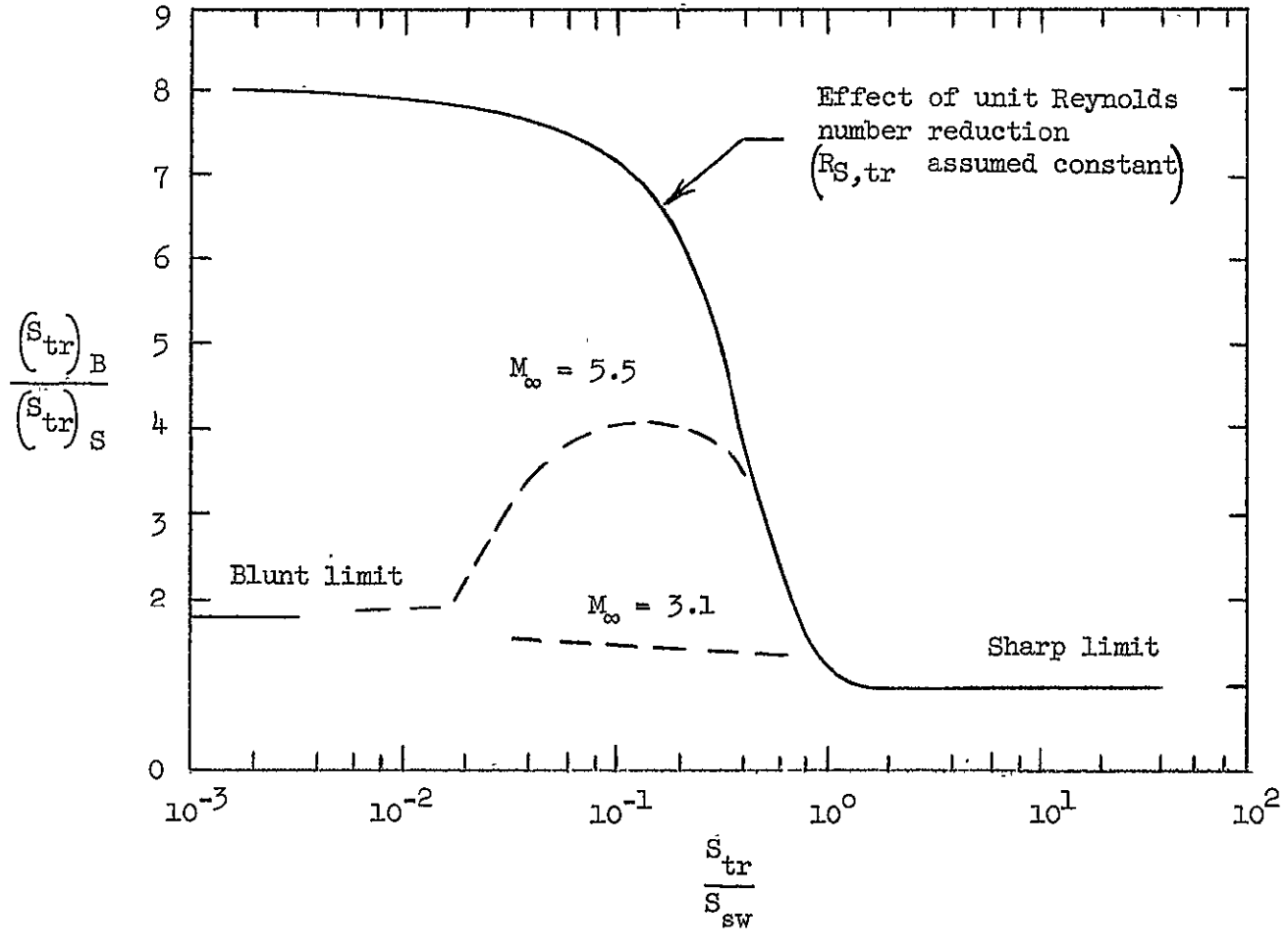

Figure 16.- Effect of nose bluntness on transition location.